



UNIVERSITY OF TRENTO - Italy

**International PhD Program in Biomolecular Sciences**

**Centre for Integrative Biology**

**XXI Cycle**

**Construction and characterization of proteome-minimized  
OMVs from *E. coli* and their exploitation in infectious  
disease and cancer vaccines**

**Tutor/Advisor**

Guido Grandi

*CIBIO - University of Trento*

**Ph.D. Thesis of**

Ilaria Zanella

*CIBIO - University of Trento*

Academic Year 2017- 2018

## Declaration of authorship

I, Ilaria Zanella, confirm that this is my own work or work I have done together with other members of our group and the use of all material from other sources has been properly and fully acknowledged.

*Ilaria Zanella*

# Contents

1	Abbreviations.....	5
2	List of Figures.....	6
3	List of Tables.....	7
4	Abstract.....	8
5	Introduction.....	9
5.1	A brief history of vaccination.....	9
5.2	How vaccines work.....	11
5.3	Approved adjuvants and new challenges.....	13
5.4	Outer Membrane Vesicles.....	16
5.5	Construction of KO mutants in <i>Escherichia coli</i> .....	19
6	Aim of the thesis.....	21
7	Results.....	22
7.1	Identification of <i>E. coli</i> OMV proteome.....	22
7.2	Genome editing protocol base on CRISPR/Cas9.....	25
7.3	Construction of an <i>E. coli</i> strain releasing OMVs deprived of 57 endogenous proteins.....	35
7.4	Attenuation of LPS reactogenicity in <i>E. coli</i> BL21(DE3) $\Delta$ 58.....	39
7.5	<i>E. coli</i> BL21(DE3) $\Delta$ 58 and $\Delta$ 60 strains releasing proteome-minimized OMVs show a significant increase in OMV production capacity.....	40
7.6	Expression of heterologous antigens in the strains releasing proteome-minimized OMVs.....	41
7.7	Immunogenicity of engineered OMVs from <i>E. coli</i> BL21(DE3) $\Delta$ 58 and <i>E. coli</i> BL21(DE3) $\Delta$ 60 strains.....	43
8	Discussion.....	46
9	Materials and methods.....	50
9.1	Bioinformatics.....	50
9.2	Construction of plasmids.....	50
9.3	Bacterial strains and culture conditions.....	52
9.4	Competent cell preparation.....	53
9.5	Gene knockout using CRISPR-Cas9.....	54
9.6	OMV purification and SDS-PAGE.....	54
9.7	Purification of recombinant <i>S. aureus</i> antigens.....	55
9.8	In vitro assay for human Toll Like Receptor 4 activity analysis.....	56
9.9	Flow cytometry on bacteria.....	56
9.10	Animal studies.....	57
9.11	ELISA.....	57
9.12	Intracellular cytokine staining on splenocytes.....	58
10	References.....	59
11	Publications.....	63
12	Acknowledgments.....	64



# 1 Abbreviations

OMVs	Outer Membrane Vesicles
CRISPR	Clustered Regularly Interspaced Short Palindromic Repeats
Cas9	CRISPR associated protein 9
DCs	Dendritic cells
dDNA	Donor DNA
DSB	Double strand break
ds-dDNA	Double strand donor DNA
dsDNA	Double strand DNA
gDNA	Guide DNA
HTP	High throughput
Ld-ss-dDNA	Single strand donor DNA targeting the leading strand
Lg-ss-dDNA	Single strand donor DNA targeting the lagging strand
LPS	Lipopolysaccharide
MAMPs	Microbe-Associated-Molecular Patterns
MHC	Major Histocompatibility Complexes
MLP	Monophosphoryl lipid A
OPV	Oral polio vaccine
PAM	Proto-spacer adjacent motif
PRRs	Pattern recognition receptors
ss-dDNA	Single strand donor DNA
ssDNA	Single strand DNA
TLRs	Toll like receptors

## 2 List of Figures

<b>Figures</b>	<b>Page</b>
Figure 1: Stimulation of the innate and adaptive immune system by adjuvant	12
Figure 2: Time line of approved adjuvants for human use	15
Figure 3: Outer Membrane Vesicles biogenesis and composition	16
Figure 4: Overview of CRISPR/Cas9 genome editing strategy in <i>Escherichia coli</i>	26
Figure 5: Selection of gDNAs for mutation of <i>ompF</i> , <i>lpp</i> and <i>fecA</i> genes	28
Figure 6: Validation of 30 bp deletions on 78 genes	31
Figure 7: Representation of the stepwise approach used to isolate strains carrying multiple mutations	33
Figure 8: CRISPR/Cas9-based protocol for simultaneous two-gene deletions	34
Figure 9: Creation and characterization of <i>E. coli</i> BL21(DE3) $\Delta$ 58 strain	36
Figure 10: Agarose gel showing PCR amplified fragments of all 58 genes mutated in <i>E. coli</i> BL21(DE3) $\Delta$ 58	37
Figure 11: Silver stained 2DE gels of OMVs from BL21(DE3) $\Delta$ <i>ompA</i> and $\Delta$ 58 strains	38
Figure 12: Schematic overview of hexacylated and pentacylated LPS	39
Figure 13: hTLR4 activation analysis by OMVs from <i>E. coli</i> BL21(DE3) $\Delta$ <i>ompA</i> , <i>E. coli</i> BL21(DE3) $\Delta$ 58 and <i>E. coli</i> BL21(DE3) $\Delta$ 60	40
Figure 14: Analysis of growth kinetic and OMV productivity for <i>E. coli</i> BL21(DE3) $\Delta$ <i>ompA</i> , <i>E. coli</i> BL21(DE3) $\Delta$ 58 and <i>E. coli</i> BL21(DE3) $\Delta$ 58 in the bioreactor	41
Figure 15: Heterologous antigens are exposed on the surface of <i>E. coli</i> BL21(DE3) $\Delta$ <i>ompA</i> and <i>E. coli</i> BL21(DE3) $\Delta$ 58	42
Figure 16: Efficient expression of heterologous antigens in OMVs derived from <i>E. coli</i> BL21(DE3) $\Delta$ 58 and $\Delta$ 60 strains	43
Figure 17: Antigen-specific IgG titers from mice sera elicited by immunization with OMVs from <i>E. coli</i> BL21(DE3) $\Delta$ 58 and $\Delta$ 60 strains expressing either FhuD2, Luke, SpA or D8-FAT1	44
Figure 18: OMVs derived from <i>E. coli</i> BL21(DE3) $\Delta$ 58 or $\Delta$ 60(pET-Lpp-fhuD2 OVA 3x) elicit specific CD8 T cell response	44

### 3 List of Tables

<b>Tables</b>	<b>Page</b>
Table 1: Approved and in clinical trials adjuvants	14
Table 2: List of 90 selected OMV-related proteins	23
Table 3: Influence of type of donor DNA (dDNA) (Lg-ss-dDNAs, Ld-ss-dDNAs, ds-dDNA) length of dDNA, concentration of dDNA and size of deletion on mutagenesis efficiency at four chromosomal loci	29
Table 4: Efficiency of simultaneous two-loci mutagenesis (ompF 5'/ompF 3' regions and fecA/lpp genes) using pCRISPR plasmids carrying repeat-gDNA1-repeat-gDNA2-repeat cassette	35
Table 5: Primers for antigens fusion to the Lpp Leader sequence and cloning into pET21B	51
Table 6: Oligos used to assemble the synthetic D8-FAT1 minigene	52
Table 7: Primers to insert D8-FAT1 minigene gene into pET21-Fhbp and pET21-FhuD2	52
Table 8: Primers to insert OVA mini gene into pET21-FhuD2	52

## 4 Abstract

Bacterial Outer Membrane Vesicles (OMVs) are naturally produced by all Gram-negative bacteria and play a key role in their biology and pathogenesis. Over the last few years, OMVs have become an increasingly attractive vaccine platform for three main reasons. First, they contain several Microbe-Associated-Molecular Patterns (MAMPs), crucial for stimulating innate immunity and promoting adaptive immune responses. Second, they can be easily purified from the culture supernatant, thus making their production process inexpensive and scalable. Third, OMVs can be engineered with foreign antigens. However, the OMV platform requires some optimization for a full-blown exploitation. First, OMVs carry a number of endogenous proteins that would be useful to eliminate to avoid possible interference of immune responses toward the vaccine antigens. Second, OMVs carry abundant quantities of lipopolysaccharide (LPS). LPS is a potent stimulator of the immune system, therefore is essential for OMV adjuvanticity, but such adjuvanticity has to be modulated to avoid reactogenicity. In this study, we have addressed the two issues by creating a strain releasing OMVs with a minimal amount of endogenous proteins and containing a detoxified LPS. In particular, we first developed a CRISPR/Cas9-based genome editing tool which allows the inactivation of any “dispensable” gene in two working days. The efficacy and robustness of this tool was validated on 78 “dispensable genes”. Using our CRISPR/Cas9 protocol, an OMV proteome-minimized *E. coli* strain, named *E. coli* BL21(DE3) $\Delta$ 58, deprived of 58 OMV associated proteins was created. We demonstrated that *E. coli* BL21(DE3) $\Delta$ 58 had growth kinetics similar to the progenitor strain and featured a remarkable increase in OMV production. Two additional genes involved in the LPS biosynthetic pathway (*msbB* and *pagP*) were subsequently inactivated creating *E. coli* BL21(DE3) $\Delta$ 60 which released OMVs with a substantially reduced reactogenicity. The exploitation of the two strains in vaccine applications was finally validated. We successfully engineered *E. coli* BL21(DE3) $\Delta$ 58 and *E. coli* BL21(DE3) $\Delta$ 60 with several different antigens, demonstrating that such antigens compartmentalized with high efficiency in the OMVs. We also demonstrated that the engineered OMVs from *E. coli* BL21(DE3) $\Delta$ 58 and *E. coli* BL21(DE3) $\Delta$ 60-derived OMVs elicited high antigen-specific antibody and T cell responses.

## 5 Introduction

### 5.1 A brief history of vaccination

The evidence, described more than 2.500 years ago by the Greek historian Thucydides (429 BC), that people who recovered from smallpox plaques rarely re-experienced the disease, constitutes the ground of modern Vaccinology. Indeed, such evidence made ancient physicians and sorcerers believe that the pustules appearing on the skins of smallpox patients not only represented the signs of the disease but also contained the “magic recipe” which protected patients from re-infection. Therefore, over the centuries, pioneer vaccinologists devised different strategies to manipulate pustule extracts to be subsequently administered to healthy people and protect them during epidemics. The first written documents on successful vaccination date back to 1000 A. D. in China, where variola scabs were exposed to air or heat and insufflated into the nose of people as immunization strategy against smallpox<sup>1</sup>. The practice of inoculation, from Latin *inoculare* which means “to graft”, was performed not only in China but most likely in other countries, including Africa and India<sup>2</sup>.

Vaccination was introduced in Europe by Lady Mary Wortley Montagu, wife of the English ambassador Edward Wortley Montagu. The family lived in Turkey in 1716 where she witnessed the inoculation practice and once returned to England she inoculated her daughter in front of the scrutiny of the Royal Society’s Physicians<sup>2</sup>. The practice started to gain popularity until few cases of death occurred after inoculation. Clearly, the pre-treatment of the vaccine was very rudimental and sometimes insufficient to fully inactivate the “unknown”, with the consequence that the inoculated people could become infected and source of disease transmission. As a consequence, the practice was abandoned for some time.

The procedure was subsequently re-adopted in 1751-1753 during a severe smallpox epidemic and was routinely used until the introduction of the safer vaccination practice developed by Edward Jenner<sup>1,3</sup>. It was common knowledge that during smallpox epidemics farmers had a much lower risk to become infected. Since cattle develop a disease (cowpox) whose manifestation resembles smallpox for the appearance of cutaneous scabs, Edward Jenner had the intuition that if people were intentionally administrated with biological material collected from the animal lesions they could become resistant to smallpox disease. In 1796, he inoculated a young boy with cowpox and subsequently intentionally challenged the boy with

extracts of pustules from human patients. As Jenner predicted, the boy did not develop the disease<sup>3,4</sup>. In 1798, Jenner published his work, representing the first human vaccine trial ever reported, and vaccination against smallpox became a common practice and culminated in global eradication of smallpox in 1979.

In the nineteenth century, bacteria were finally discovered and microbial pathogens were associated with the insurgency of infectious diseases. Louis Pasteur was the first to develop live attenuated cholera vaccine and anthrax vaccine, after the observation that the pathogens could be made less virulent by exposure to oxygen, high temperature and chemicals<sup>5</sup>.

The practice of pathogen attenuation was further developed by Albert Calmette and Camille Guérin who used culturing in artificial media to attenuate *Mycobacterium bovis*, a bovine tuberculosis bacteria, to protect against human tuberculosis. Moreover, Max Theiler used several passages in mice and chicken embryos to attenuate Yellow fever virus<sup>6</sup> and his attenuated strain represents one of the most effective vaccines ever developed and is still routinely administered in countries where yellow fever is endemic.

In the middle of the 20<sup>th</sup> century, the cell culture was utilized to attenuate the virulence of viruses through several passages in culture<sup>2</sup>. In this period, many vaccines based on attenuated viruses, including those for poliomyelitis (polio), measles, rubella, mumps and varicella, were developed<sup>7,8,9,10</sup>. The passages in cell cultures are usually carried out at a sub-physiological temperature and lead to strain adaptation to the new culture conditions and the loss or modification of genes involved in virulence and transmission in the human host. One of the best examples is the oral polio vaccine (OPV). The attenuate poliovirus elicits protection without causing disease since it is unable to replicate efficiently in the nervous system<sup>11</sup>.

Live/attenuated OPV has been a triumph in the history of human health having almost eradicated poliomyelitis from the world. However, the OPV vaccine was not completely safe: in one out of 3 million vaccines the attenuated virus can revert to the wild type form and become virulent and infective<sup>11</sup>. For this reason, it has been replaced with fully inactivated vaccines and nowadays live/attenuated pathogens are rarely considered as a valid option for the development of new vaccines.

As technology advanced, it became possible to purify specific components of the pathogen of interest and use such components as vaccines. Typical examples are toxins (i.e. diphtheria, tetanus and cholera vaccines), capsular polysaccharides (i.e. Hib, pneumococcal and meningococcal vaccines) and proteins (i.e. pertussis vaccine).

In the 21<sup>st</sup> century, there are still a number of pathogens for which vaccines have not been developed yet and such pathogens represent a serious threat for human health particularly in consideration of the dramatic increase of antibiotic resistance. High throughput technologies and improved knowledge of microbial pathogenesis and immunology now offer new opportunities to identify protective antigens and to discover novel adjuvants, which can better orchestrate the effector functions of the immune system.

## 5.2 How vaccines work

To be effective vaccines should induce the same natural immunity that our organism develops in response to infection. Therefore, a rational vaccine design should stem from the knowledge of how our immune system develops natural immunity.

At the site of entry, microbes are recognized by the cells of the innate immunity, which provide immediate defense against the invasion and trigger the cascade of events leading to the adaptive immune responses (Figure 1).

The innate immune cells include phagocytic cells, such as macrophages, that not only phagocytose and kill the invaders but also release cytokines in response to the recognition, through pattern-recognition receptors (PRRs), of conserved components of the pathogens (microbial-associated molecular patterns (MAMPs)<sup>12</sup>). Cytokine release is responsible for the induction of an inflammatory response, which recruits additional phagocytic cells and initiates the adaptive immune response. The key cellular components involved in the activation of adaptive immunity are the dendritic cells (DCs). Like macrophages, DCs recognize pathogens via PRRs and release cytokines. Furthermore, they phagocytose pathogens and extracellular antigens by endocytosis, digest pathogen-derived proteins into small fragments (epitopes) and present such fragments on their surface in the context of the Major Histocompatibility Complexes (MHC) class I and II. Then, DCs migrate to the draining lymph nodes through the lymphatic system and present the MHC I/MHC II-bound epitopes to naïve T cells. Naive T cells thus become effector CD4<sup>+</sup> and CD8<sup>+</sup> T cells. Effector CD4<sup>+</sup> T cells stimulate the production

of pathogen-specific antibodies and migrate to the site of infection where they exert their effector functions by potentiating the phagocytic activity of phagocytic cells. Effector CD8+ T cells also reach the infection site, but they function by directly killing cells infected by intracellular pathogens such as viruses.

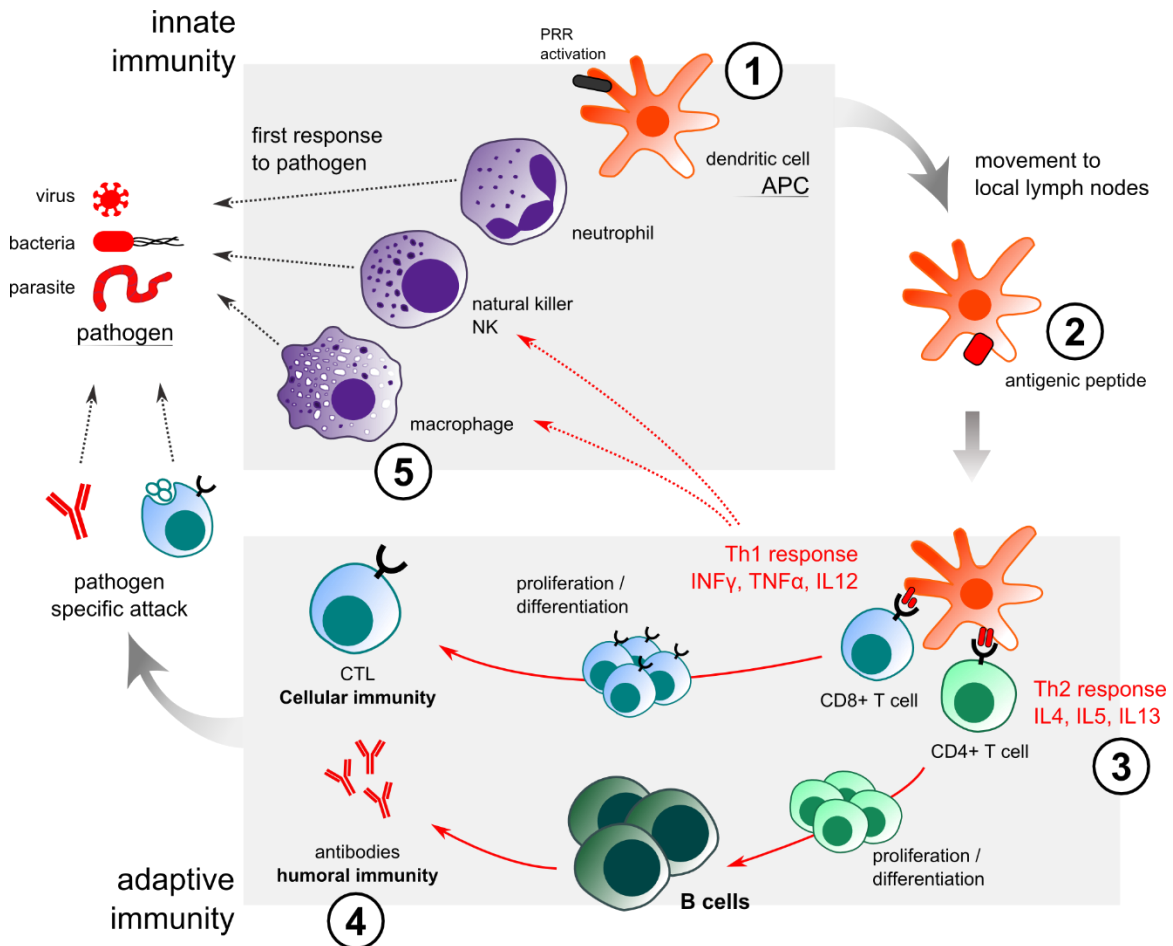


**Figure 1: Stimulation of the innate and adaptive immune system by adjuvant.** Figure taken from [www.ozbiosciences.com](http://www.ozbiosciences.com). (1) recruitment of APC at the injection site. (2) enhancement of antigen uptake. (3) enhancement of Th2 response. (4) enhancement of humoral immune response. (5) improvement of NALP3/inflammasome in mac.

Antibodies, produced by B cells after stimulation by effector CD4+ T cells, exert anti-microbial activity through different mechanisms. First, they can bind to secreted toxins and neutralize their toxic action. Second, antibodies can bind the pathogen and prevents its interaction with host cells and tissues. Third, antibodies bound to the pathogen are recognized by receptors on phagocytic cells, thus facilitating phagocytosis. Forth, antibodies can activate the complement system, which leads to the direct lysis of bacteria or to pathogen phagocytosis.

Finally, antibodies can bind the surface of infected cells which are killed by NK cells, a process known as antibody-dependent cell-mediated cytotoxicity (ADCC)<sup>13</sup>.

As said above, a key step for the activation of adaptive immunity is the recognition of MAMPs by PRRs, the best characterized of which are the Toll-like receptors (TLRs) and NOD-like receptors (NLRs). TLRs have a central role in sensing different MAMPs, including unmethylated double-stranded DNA (CpG), single- and double-stranded RNA, lipoproteins, lipopolysaccharide (LPS), peptidoglycan, and flagella<sup>14,15</sup>. PRR activation stimulates the release of cytokine and chemokines<sup>16,17</sup>. It is important to underline that PRRs dictate the profile of cytokines released by immune cells and consequently the type of adaptive immunity that is necessary to eliminate the specific pathogen. For instance, extracellular bacteria stimulate the release of IL17 and IL23 which promote recruitment and killing capacity of phagocytic cells while viruses stimulate the release of IFN $\gamma$  which elicits cytotoxic CD8+ T cells.

According to these mechanisms, it appears that effective vaccines have to be tailored to induce the proper immune response required to eliminate the specific pathogens they are made for. Moreover, it becomes clear why vaccines based on attenuated viruses, such as yellow fever, measles and polio OPV vaccines, are generally very effective: being alive and non-virulent copies of their progenitors they elicit exactly what is needed in terms of quality, quantity, and location of immune responses. Furthermore, the above also explains why subunit-based vaccines, in addition to contain proper antigens, should include specific components, known as adjuvants, which by stimulating the correct PRRs activate the type of immune response necessary to prevent infection.

### 5.3 Approved adjuvants and new challenges

The importance of adjuvants was recognized very early in vaccination. As introduced earlier, the first written document of successful vaccination come from the China of 1000 A.D. They had the intuition to formulate a mixture of variola scabs from mildly affected patients, stored for at least 1 month, with *Uvularia grandiflora* in a 4:1 ratio before intranasal inoculation. Therefore, *Uvularia grandiflora* can be considered as the first attempt at using an adjuvant.

In modern vaccinology, the first molecules to be used as adjuvants were phosphate or hydroxide salts of aluminium (known as alum). Alum was originally discovered as a good antigen delivery system and in 1926 Glenny and Pope showed that alum-absorbed diphtheria

toxoid was a more potent vaccine compared to the antigen alone<sup>18</sup>. Although the mode of action is still not exactly clear, it is now understood that alum increases antigen uptake by APCs at the site of injection. In addition, alum stimulates NALP3 Inflammasome complex, which is required for the processing of several pro-inflammatory cytokines that ultimately activate inflammatory DCs capable of priming T cells<sup>19</sup>. Alum was first approved for tetanus and diphtheria toxoids vaccines and it is currently formulated in one-third of the vaccines present on the market<sup>20</sup>. Interestingly, no other adjuvant for human use was introduced for several decades (Figure 2), until 1997 when MF59 was licensed as a part of vaccines against pandemic influenza strains such as H5N1 or H7N9<sup>21</sup>. MF59 is an oil-in-water emulsion prepared with squalene and biodegradable/biocompatible oil<sup>22</sup>. Like alum, MF59 is a delivery system. Furthermore, it appears that MF59 has the ability to upregulate the production of cytokines and chemokines which attract APCs to the site of injection increasing antigen uptake and subsequent transport to draining lymph node<sup>23</sup>. AS03 is another squalene-based emulsion with the addition of Alpha-tocopherol (vitamin E) licensed in 2009. Despite their success, all these adjuvants are not potent inducers of cytotoxic T cell responses and therefore they are not very effective against intracellular pathogens and cancer.

**Table 1: Approved and in clinical trials adjuvants (from Luis A. Brito, Derek T. O'Hagan, 2014)**

Adjuvant	Description	Clinical status
Aluminum salts	Insoluble aluminum salts e.g., phosphates and hydroxides. Have an extensive safety record and are being used as a platform for second generation adjuvants. Antigens are typically adsorbed to the surface.	Licensed in US and EU
MF59	Squalene oil in water emulsion adjuvant that has been part of a licensed flu vaccine since 1997. Antigens are not associated with emulsion droplets. Extensive safety record.	Licensed in EU
AS03	Squalene oil in water emulsion adjuvant with the added immune potentiator alpha tocopherol, used in flu vaccines during 2009 pandemic, but associated with narcolepsy.	Licensed in EU and US
AS04	Combination of aluminum adjuvant with the TLR 4 agonist monophosphoryl Lipid A (MPL) co-adsorbed. Approved as a licensed HPV vaccine (Cervarix)	Licensed in EU and US
Virosomes	Influenza virus envelopes reconstituted in phosphatidylcholine bilayers (virosomes).	Licensed in EU
AS01	Liposomes composed of dioleoylphosphatidylcholine (DOPC), cholesterol, MPL and QS21 in a 20 : 5 : 1 : 1 (w/w) ratio.	Phase III Malaria
CAF01	Cationic liposome composed of dimethyldioctadecylammonium bromide (DDA), and the glycolipid trehalose 6,6'-dibehenate (TDB) in a 5:1 (w/w) ratio prepared by film hydration.	Phase I
Poly I:C	Synthetic double stranded oligonucleotide containing repeating units of inosine and cytosine that signals through TLR3.	Phase I
IC31	Antimicrobial peptide KLK bound to ODN1a, signals through TLR9.	Phase I
AS02	Co-mixture of AS03 emulsion adjuvant with QS21 and MPL.	Phase II
Imiquimod	Small molecules immune potentiators that signal through TLR7/8.	Phase II
CpG oligonucleotides (ISS 1018)	TLR9 agonists based on bacterial DNA.	Phase III
SE/SE-GLA	Squalene based emulsion that is a stand-alone emulsion adjuvant, or combined with the TLR4 agonist GLA.	Phase I
ISCOMS and ISCOMATRIX	Small (40 nm) lipid based adjuvants consisting of phospholipids, cholesterol and saponins.	Phase I

The discovery that changed the game of adjuvant formulation and raised the potential of developing novel adjuvants was the understanding of innate immune receptors such as TLRs and nucleotide-binding oligomerization domain-like receptors (NLR). Agonists of hTLR4 have become important adjuvants and are being tested for cancer treatments. One such agonist is monophosphoryl lipid A (MPL), purified from *Salmonella Minnesota* LPS<sup>24</sup>. MLP was combined with Alum to formulate AS04, an adjuvant used for licensed human vaccine preventing human

papillomavirus (HPV)<sup>25</sup>. The combination of MPL/alum adjuvant enhances both effector and memory B-cell immunity<sup>26</sup>. The stimulation of hTLR4 results in the production of IL-12 and increased expression of MHC class II and costimulatory molecules. Many others PRR agonists have been studied, such oligonucleotides containing CpG motifs (CpG ODN). They act by binding the intracellular TLR9, expressed in the vesicular compartment of immune cells. CpG ODN have been extensively studied in clinical trials as powerful inducers of Th1, including antibody and antigen-specific T cell production<sup>27</sup>. Other examples are imiquimod (R837), resiquimod (R848) and 3M-052, synthetic TLR7/8 agonists reported to exert potent adjuvant activities by inducing robust antigen-specific humoral and Th1 type cellular immunity. TLR agonists have been so far proved to be effective adjuvants with some molecules licensed for human use and many others in clinical trials for use in both vaccines against pathogens and cancer vaccines.

**Time line of licensed adjuvants in EU**

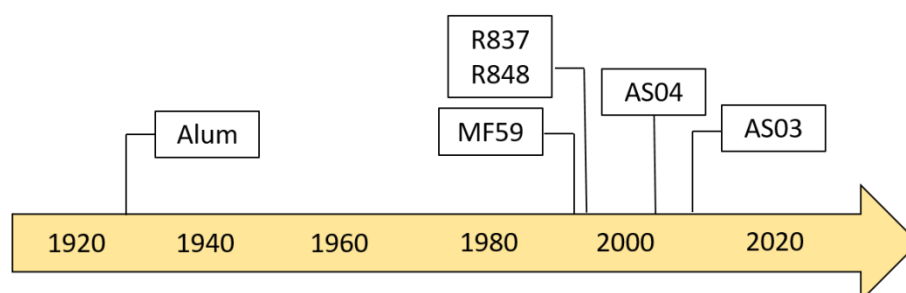


**Figure 2: Time line of approved adjuvants for human use.**

A new pathway that has been investigated recently as a candidate vaccine adjuvant is STING (STimulator of INterferon Genes). STING is an endoplasmic reticulum transmembrane protein belonging to the family of nucleic acid sensors<sup>28</sup>. It is activated by cytosolic dsDNA from pathogens or self-DNA from stressed or damaged cells in cyclic GMP-AMP synthase (cGAS) dependent manner. Cytosolic DNA is detected by cGAS, it functions as a second messenger that binds and activates STING. STING activation triggers TBK-1/IRF-3 signaling cascades inducing the expression IFN- $\beta$  as well IKK/NF $\kappa$ B-dependent upregulation of inflammatory cytokines and chemokines<sup>29</sup>. In preclinical models the use of c-GMP have shown good results, c-di-GMP injected intratumorally demonstrated to induce caspase 3-dependent apoptosis of tumor cells and release of tumor-associated antigens promoting DCs activation and CD8+ T-

cell responses against those antigens<sup>27</sup>. At present, one STING agonist, 5,6-dimethylxanthenone-4-acetic acid (DMXAA)<sup>30</sup>, has reached the clinics.

#### 5.4 Outer Membrane Vesicles

More than 50 years ago, researchers observed that Gram-negative bacteria secrete OMVs<sup>31</sup>. However, only the last 15 to 20 years have brought a greater understanding of the regulation and function of vesiculation. OMVs are closed spheroid particles of heterogeneous size, 50-300 nm in diameter, generated through a “budding out” of the bacterial outer membrane and, consistently, the majority of their components are represented by LPS, glycerophospholipids, outer membrane proteins and periplasmic proteins<sup>31,32</sup> (Figure 3).

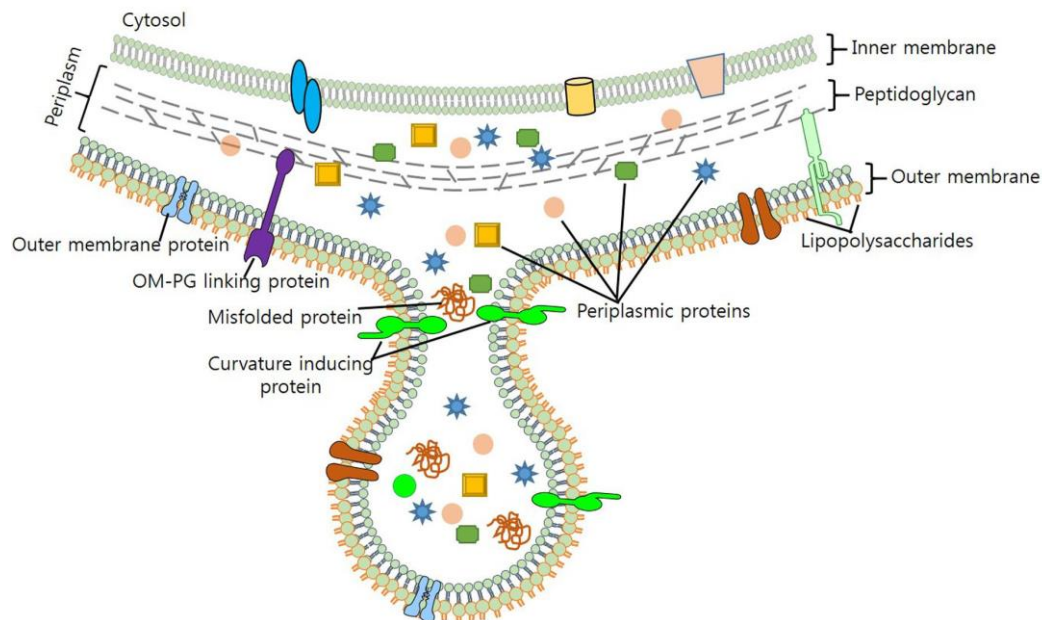


**Figure 3: Outer Membrane Vesicles biogenesis and composition** (from Jan et al., 2017).

OMVs represent a distinct secretory pathway with a multitude of functions, including inter and intra species cell-to-cell cross-talk, biofilm formation, genetic transformation, defense against host immune responses, and toxin and virulence factor delivery to host cells<sup>32,33</sup>. OMVs interaction to host cells can occur by endocytosis after binding to host cell receptors or lipid rafts. Alternatively, OMVs have been reported to fuse to host cell membrane, leading to the direct release of their content into the cytoplasm of the host cells<sup>34</sup>.

OMVs purified from several pathogens, including *Neisseria*, *Salmonella*, *Pseudomonas*, *Vibrio cholerae*, *Burkholderia*, and *E. coli*<sup>35,36,37</sup>, induce potent protective immune responses against the pathogens they derive from, and highly effective anti-*Neisseria* OMV-based vaccines are already available for human use<sup>38</sup>. Such remarkable protection is attributed to three key features of OMVs. First, they are readily phagocytosed by professional antigen-presenting cells, which get activated and present OMV-derived peptides on MHC class II and MHC class I. Second, they carry the proper immunogenic antigens, which, in extracellular pathogens, usually reside on the surface and therefore are naturally incorporated in OMVs. Indeed, OMV immunization induces potent antibody responses against the major membrane-associated antigens. However, OMV immunogenicity is not restricted to antibody responses. For instance, mice immunized with *Salmonella* OMVs develop robust *Salmonella*-specific B and T cell responses, and OMVs stimulate IFN- $\gamma$  production by a large proportion of CD4<sup>+</sup> T cells from mice previously infected with *Salmonella*, indicating that OMVs are an abundant source of antigens recognized by *Salmonella*-specific CD4<sup>+</sup> T cells<sup>35</sup>. Third, and most importantly, OMVs carry several MAMPs which, by binding to PRRs, play a key role in stimulating innate immunity and promoting adaptive immune responses. OMV-associated MAMPs include LPS which, in concert with MD-2 and CD14, binds TLR-4, lipoproteins, which interact with TLR-2, and peptidoglycan, which binds to intracellular NOD1<sup>39</sup>. Engagement of this group of PRRs results in the expression of cytokines through the activation of NF- $\kappa$ B transcription factor. Interestingly, LPS, lipoproteins and peptidoglycan can work synergistically, thus potentiating the built-in adjuvanticity of OMVs<sup>40</sup>.

Two additional key features make OMVs particularly attractive for vaccine applications. First, several studies have demonstrated that OMV protein content can be manipulated by genetic engineering. Kesty and Kuehn demonstrated that *Yersinia enterocolitica* outer membrane protein Ail assembled on OMVs surface when expressed in *E. coli*, and that the GFP fluorescence protein fused to the “twin arginine translocation (TAT)” signal sequence was incorporated in the OMV lumen<sup>41</sup>. Furthermore, a number of heterologous proteins have been successfully exported to the surface of OMVs when fused to the  $\beta$ -barrel forming autotransporter AIDA and the hemolysin ClyA, two proteins that naturally compartmentalized in *E. coli* OMVs<sup>42</sup>. In our laboratory, we have devised effective strategies to incorporate heterologous antigens in the lumen of OMVs<sup>43</sup> and in their membrane (Irene et. al, manuscript submitted) and we have shown that foreign polypeptides can be delivered to the OMV surface by fusing them to lipoproteins<sup>44</sup>. Second, using hyper-vesiculating mutant strains, OMVs can

be easily purified from the culture supernatant and their purification process can be promptly scaled-up from the laboratory to industrial levels<sup>44,43,45,46</sup>. Once the supernatant is separated from the biomass, the purification of the vesicles can be carried out using tangential flow filtration with production yield higher than 100 mg of vesicles (protein content) per liter of culture<sup>47</sup> under GMP conditions.

In conclusion, OMVs represent a promising vaccine platform due to their built-in adjuvanticity, the possibility of manipulation and simplicity of the production process.

For a full-blown development of OMVs as vaccine platform, three potential limitations have to be overcome.

First, as said above, OMVs have remarkable adjuvanticity properties thanks to the presence of several MAMPs, which, stimulate different innate immunity receptors. In particular, LPS is present in OMVs at a concentration of approximately 0.5 mg per mg of total OMV proteins<sup>48</sup> and by binding to TLR4, LPS substantially contributes to adjuvanticity. However, LPS abundance is also responsible for OMV reactogenicity, which has to be reduced for human use. A number of mutations in the LPS biosynthetic pathway have been described that reduce the TLR4 agonistic activity of LPS by removing acyl chains to the hexa-acylated lipid A moiety. They include the inactivation of the acyl-transferase genes *msbB* and *pagP* which results in the synthesis of a LPS carrying a penta-acylated lipid A<sup>49,50</sup>. In our laboratory, we have also exploited the inactivation of genes involved in the LPS biosynthetic pathway to modulate adjuvanticity/reactogenicity of OMVs (manuscript submitted).

Second, as already pointed out, the possibility of being manipulated makes OMVs particularly attractive for vaccine applications and several strategies have been devised to decorate OMVs with heterologous antigens. The ideal system should (i) be highly flexible, allowing OMV compartmentalization of most heterologous antigens, and (ii) result in the accumulation of sufficiently large quantities of heterologous antigens, allowing the elicitation of proper anti-antigen immune responses. The development of novel OMV engineering strategies is an active field of translational research and our laboratory is particularly active on this line of activity.

Third, proteomic data indicate that OMVs incorporate approximately 100-150 major endogenous proteins present in the outer membrane and periplasmic compartments of the OMV producing strains<sup>51,52,53</sup>. All these proteins are potentially immunogenic and therefore

could “dilute” or even partially suppress the immune responses against the desired antigens. Therefore, the availability of mutant strains which release OMVs with a minimal amount of endogenous proteins would be highly desirable. *This later aspect has been the major interest of my PhD experimental work which has been focused on the systematic inactivation of the genes encoding a large set of proteins present in the OMVs released by E. coli BL21(DE3) strain.*

## 5.5 Construction of KO mutants in *Escherichia coli*

Being *E. coli* one of the most extensively studied organisms on earth for both scientific and translational purposes, several procedures have been described for gene knock-out and knock-in.

Currently, there are three main approaches for manipulation of chromosomal DNA in *E. coli*, all utilizing phage recombinase-mediated homologous recombination (recombineering), using either the  $\lambda$  Rac prophage system<sup>54,55</sup> or the three bacteriophage  $\lambda$  Red proteins Exo, Beta, and Gam<sup>56,57</sup>.

The first approach envisages the creation of knockout mutants by fusing at the 5’ and 3’ ends of an antibiotic resistance marker gene (or other selection markers) PCR products preceding and following the target gene, respectively. Mutant colonies are isolated in the appropriate selective medium after transformation with linear or circular constructs. The selection marker is subsequently eliminated by counter-selection, leaving a “scarless” chromosomal mutation<sup>58</sup>.

In a second approach, Court and co-workers demonstrated that chromosomal gene mutations can be achieved without the need of selection markers and using synthetic single stranded DNAs (ss-DNAs) or double stranded DNAs (ds-DNAs), which anneal to their complementary chromosomal regions and mediate gene modification<sup>59</sup>.

The third approach, proposed for the first time by Jiang and co-workers<sup>60</sup>, makes use of the CRISPR/Cas9 technology. Briefly, the Cas9 nuclease and the  $\lambda$  Red machinery are genetically introduced in the strain to be modified and subsequently the strain is co-transformed with a plasmid (pCRISPR) encoding the guide RNA, which promotes the site-specific DNA cleavage by the Cas9, and donor DNA (PCR-derived or chemically synthesized) partially homologous to the cleaved extremities. This allows the  $\lambda$  Red-mediated repair of the cleavage site with the concomitant introduction of the desired mutation.

While effective, the first two approaches are not ideal for high-throughput applications since they are laborious and time-consuming (in the case of the first approach) <sup>58</sup> and feature mutagenesis efficiencies often below 1% (in the case of the second approach)<sup>59</sup>. On the contrary, the third approach was shown to lead to efficiencies as high as 50-80%<sup>61,62,63</sup>.

However, one aspect of the CRISPR/Cas9 technology that still remained to be thoroughly addressed was the “robustness” of the strategy defined as the success rate of mutated loci with respect to the number of mutations attempted. Knowing the robustness of the specific CRISPR/Cas9-based protocol in use is particularly relevant in high-throughput applications, where the repetition of mutagenesis experiments and/or the analysis of large numbers of colonies would be impractical.

## 6 Aim of the thesis

One of the main tasks of our Synthetic and Structural Vaccinology Laboratory at the University of Trento, is to exploit the potentiality of OMVs as a vaccine-platform. As already pointed out, OMVs have an intrinsic adjuvanticity, can be engineered to express heterologous antigens and are easy to produce. However, the presence of *E. coli* endogenous proteins might affect and dilute the immune response against the heterologous antigens engineered in OMVs. To mitigate this effect, we decided to reduce the repertoire of homologous proteins present in the OMV compartment by systematically knocking out the corresponding genes from the OMV-producing strains.

The aims of my thesis can be summarized as follows:

1. Identification and selection the OMV endogenous proteins to be deleted
2. Development of a highly efficient and robust genome editing protocol based on CRISPR/Cas9 technology to delete dispensable OMV proteins
3. Creation of *E. coli* strains releasing proteome–minimized OMVs, using the gene editing platform developed in point 2, and characterization of their growth kinetics and OMV production
4. Analysis of the expression of heterologous antigens in the OMVs released by the genetically modified strains
5. Analysis of antigen-specific antibody and T cell responses induced by proteome-minimized OMVs

This activity has so far led to the publication of one paper (Zerbini et al., 2017) of which I am the second author. A second paper, which I will be the first author of, is under submission.

I also wish to point out that in addition to my main research project I have been involved in other activities related to the exploitation of OMVs as vaccines. Such activities have been documented in three scientific publications (L. Fantappie' et al., 2017; A. Grandi et al. 2017; A. Grandi et al. 2018) of which I am a co-author.

## 7 Results

As pointed out in the “Aim of the Thesis” the main objectives of my experimental work was 1) to reduce the repertoire of homologous proteins present in the OMV compartment thus generating “proteome-minimized OMVs”, and 2) to test the proteome-minimized OMVs as a vaccine platform.

To reach these objectives, the experimental work has been articulated in the following activities:

- Identification and selection of the OMV endogenous proteins
- Development of a highly efficient and robust genome editing protocol
- Creation of *E. coli* strains releasing proteome–minimized OMVs
- Analysis of the expression of heterologous antigens in proteome-minimized OMVs
- Analysis of antigen-specific antibody and T cell responses induced by proteome-minimized OMVs

### 7.1 Identification of *E. coli* OMV proteome

The composition of OMV proteins was determined in two ways.

First, purified *E. coli* BL21 $\Delta$ *ompA*–derived OMVs were separated by 2D gel electrophoresis (2DE) and protein spots were picked and characterized by MALDI-TOF-TOF Mass Spectrometry. A total of 114 unique sequences were identified corresponding to 69 unique *E. coli* proteins<sup>44</sup>.

Second, bioinformatics analysis of total *E. coli* predicted proteins was carried out using different algorithms (Proteome Analyst, SOSUI-GramN and PSORTb version 3.0.2) to predict periplasmic and outer membrane proteins. These proteins are those which are expected to be found in the OMV compartment. The in-silico analysis predicted 504 *E. coli* proteins localized in the outer membrane (OM) or in the periplasm (P) of *E. coli*. Interestingly and as expected, all 69 proteins experimentally identified by 2D-gel mass spectrometry were included in the *in silico* predicted proteins, with the exception for *tuf1*, elongation factor Tu 1, and *pdxB*, erythronate-4-phosphate dehydrogenase, encoded proteins and YghJ, a hypothetical inner-membrane protein.

Once the OMV proteome was defined, we next selected among the 504 proteins those whose deletion should be attempted to create a mutant strain releasing proteome-minimized OMVs. The selection was carried out in two steps. First, the “essential proteins” included in the 504 protein list were eliminated by inspecting the Keio collection, a database in which all *viable* and *non-viable* single-gene knockout *E. coli* K-12 mutations are reported. Second, we ranked the dispensable proteins on the basis of their predicted or experimentally verified level of expression, with the idea to focus our attention on the most abundant ones. This combined approach led us to define the list of 90 proteins reported in Table 2. These proteins have been the focus of our genome editing activity.

**Table 2: List of 90 selected OMV-related proteins.** For each protein a UniProt accession number has been assigned with its annotation.

<b>UniProt Accession number</b>	<b>gene name</b>	<b>Annotation (according to UniProt)</b>
P19926	<a href="#">agp</a>	Glucose-1-phosphatase
P45565	<a href="#">ais</a>	Lipopolysaccharide core heptose(II)-phosphate phosphatase
P30859	<a href="#">artI</a>	Putative ABC transporter arginine-binding protein 2
P30860	<a href="#">artJ</a>	ABC transporter arginine-binding protein 1
P77774	<a href="#">bamB</a>	Outer membrane protein assembly factor BamB
P0A903	<a href="#">bamC</a>	Outer membrane protein assembly factor BamC
P0A937	<a href="#">bamE</a>	Outer membrane protein assembly factor BamE
P37650	<a href="#">bcsC</a>	Cellulose synthase operon protein C
P33363	<a href="#">bglX</a>	Periplasmic beta-glucosidase
P0AB40	<a href="#">bhsA</a>	Multiple stress resistance protein BhsA
P77330	<a href="#">borD</a>	Prophage lipoprotein Bor homolog
P17315	<a href="#">cirA</a>	Colicin I receptor
P45955	<a href="#">cpoB</a>	Cell division coordinator CpoB
P0C0V0	<a href="#">degP</a>	Periplasmic serine endoprotease DegP
P39099	<a href="#">degQ</a>	Periplasmic pH-dependent serine endoprotease DegQ
P0AEG6	<a href="#">dsbC</a>	Thiol:disulfide interchange protein DsbC
P0ADB7	<a href="#">ecnB</a>	Entericidin B
P23827	<a href="#">eco</a>	Ecotin
P0AB24	<a href="#">efeO</a>	Iron uptake system component EfeO
P0C960	<a href="#">emtA</a>	Endo-type membrane-bound lytic murein transglycosylase A
P10384	<a href="#">fadL</a>	Long-chain fatty acid transport protein
P13036	<a href="#">fecA</a>	Fe(3+) dicitrate transport protein FecA
P05825	<a href="#">fepA</a>	Ferrienterobactin receptor
P06971	<a href="#">fhuA</a>	Ferrichrome outer membrane transporter/phage receptor
P45523	<a href="#">fkpA</a>	FKBP-type peptidyl-prolyl cis-trans isomerase FkpA

P26648	<a href="#">ftsP</a>	Cell division protein FtsP
P0AEQ3	<a href="#">glnH</a>	Glutamine-binding periplasmic protein
P09394	<a href="#">glpQ</a>	Glycerophosphodiester phosphodiesterase, periplasmic
P37902	<a href="#">gltI</a>	Glutamate/aspartate import solute-binding protein
P0AEU0	<a href="#">hisJ</a>	Histidine-binding periplasmic protein
Q03961	<a href="#">kpsD</a>	Polysialic acid transport protein KpsD
P02943	<a href="#">lamB</a>	Maltoporin
P25894	<a href="#">loiP</a>	Metalloprotease LoiP
P45464	<a href="#">lpoA</a>	Penicillin-binding protein activator LpoA
P0AB38	<a href="#">lpoB</a>	Penicillin-binding protein activator LpoB
P69776	<a href="#">lpp</a>	Major outer membrane prolipoprotein Lpp
P0AEX9	<a href="#">malE</a>	Maltose/maltodextrin-binding periplasmic protein
P03841	<a href="#">malM</a>	Maltose operon periplasmic protein
P40120	<a href="#">mdoD</a>	Glucans biosynthesis protein D
P33136	<a href="#">mdoG</a>	Glucans biosynthesis protein G
P0A908	<a href="#">mipA</a>	MltA-interacting protein
P76506	<a href="#">mlaA</a>	Intermembrane phospholipid transport system lipoprotein MlaA
P0ADV7	<a href="#">mlaC</a>	Intermembrane phospholipid transport system binding protein MlaC
P0A935	<a href="#">mltA</a>	Membrane-bound lytic murein transglycosylase A
P0ADA3	<a href="#">nlpD</a>	Murein hydrolase activator NlpD
P40710	<a href="#">nlpE</a>	Lipoprotein NlpE
P21420	<a href="#">nmpC</a>	Putative outer membrane porin protein NmpC
P0A910	<a href="#">ompA</a>	Outer membrane protein A
P77747	<a href="#">ompN</a>	Outer membrane protein N
P0A917	<a href="#">ompX</a>	Outer membrane protein X
P23843	<a href="#">oppA</a>	Periplasmic oligopeptide-binding protein
P0ADB1	<a href="#">osmE</a>	Osmotically-inducible putative lipoprotein OsmE
P0A912	<a href="#">pal</a>	Peptidoglycan-associated lipoprotein
P02932	<a href="#">phoE</a>	Outer membrane pore protein E
P0A921	<a href="#">pldA</a>	Phospholipase A1
P0AFK9	<a href="#">potD</a>	Spermidine/putrescine-binding periplasmic protein
P0AFL3	<a href="#">ppiA</a>	Peptidyl-prolyl cis-trans isomerase A
P23865	<a href="#">prc</a>	Tail-specific protease
P0AFM2	<a href="#">proX</a>	Glycine betaine/proline betaine-binding periplasmic protein
P05458	<a href="#">ptrA</a>	Protease 3
P69411	<a href="#">rcsF</a>	Outer membrane lipoprotein RcsF
P10100	<a href="#">rlpA</a>	Endolytic peptidoglycan transglycosylase RlpA
P0AEU7	<a href="#">skp</a>	Chaperone protein Skp
P37194	<a href="#">slp</a>	Outer membrane protein slp
P0A905	<a href="#">slyB</a>	Outer membrane lipoprotein SlyB
P0ABZ6	<a href="#">surA</a>	Chaperone SurA
P13482	<a href="#">treA</a>	Periplasmic trehalase

P0A927	<a href="#">tsx</a>	Nucleoside-specific channel-forming protein Tsx
P07024	<a href="#">ushA</a>	Protein UshA
P0ADA5	<a href="#">yajG</a>	Uncharacterized lipoprotein YajG
P77717	<a href="#">ybaY</a>	Uncharacterized lipoprotein YbaY
P0AAX8	<a href="#">ybis</a>	Probable L,D-transpeptidase YbiS
P0A8X2	<a href="#">yceI</a>	Protein YceI
P64451	<a href="#">ydcL</a>	Uncharacterized lipoprotein YdcL
P77318	<a href="#">ydeN</a>	Uncharacterized sulfatase YdeN
P76177	<a href="#">ydgH</a>	Protein YdgH
P76537	<a href="#">yfeY</a>	Uncharacterized protein YfeY
P0AD44	<a href="#">yfhG</a>	Uncharacterized protein YfhG
P65292	<a href="#">ygdI</a>	Uncharacterized lipoprotein YgdI
P65294	<a href="#">ygdR</a>	Uncharacterized lipoprotein YgdR
P0ADS6	<a href="#">yggE</a>	Uncharacterized protein YggE
P0CK95	<a href="#">yghJ</a>	Putative lipoprotein AcfD homolog
P0ADU5	<a href="#">ygiW</a>	Protein YgiW
P64614	<a href="#">yhcN</a>	Uncharacterized protein YhcN
P37648	<a href="#">yhjJ</a>	Protein YhjJ
P37665	<a href="#">yiaD</a>	Probable lipoprotein YiaD
P0ADN6	<a href="#">yifL</a>	Uncharacterized lipoprotein YifL
P0AF70	<a href="#">yjeI</a>	Uncharacterized protein YjeI
P76115	<a href="#">yncD</a>	Probable TonB-dependent receptor YncD
P76116	<a href="#">yncE</a>	Uncharacterized protein YncE
P64596	<a href="#">yraP</a>	Uncharacterized protein YraP

## 7.2 Genome editing protocol base on CRISPR/Cas9

To carry out the systematic cumulative inactivation of the 90 selected proteins, it was first necessary to build-up a robust and reliable high-throughput (HTP) genome-editing protocol. The development of such HTP protocol, which is based on the CRISPR/Cas9 technology and is described below, has been the first task of my experimental activity.

### *General description of the CRISPR/Cas9 protocol for genome editing*

The CRISPR/Cas9 protocol developed in the Synthetic and Structural Vaccinology Laboratory is composed of three elements: pCasRed plasmid, pCRISPR-*SacB*-gDNA plasmid, and the synthetic, mutation-inducing oligonucleotide (donor DNA) (Figure 4). The pCasRed plasmid and pCRISPR-*SacB*-gDNA derive respectively from pCas9 (ADDGENE # 42876) and pCRISPR plasmid (ADDGENE # 42875)<sup>64</sup>, respectively. The pCasRed carries, under the control of a constitutive promotor, (i) the Cas9 nuclease, (ii) the tracrRNA, and (iii) the Chloramphenicol resistance cassette (CmR). Furthermore and importantly, the plasmid expresses, under the

pBAD arabinose inducible promoter<sup>65</sup>, the  $\lambda$  Red (*Exo*, *Beta*, *Gam*) machinery, necessary to promote homologous recombination. The pCRISPR-*SacB*-gDNA plasmid carries the synthetic DNA fragment (gDNA) expressing the guide RNA and the *SacB* gene fused to the Kanamycin resistance gene (*Km<sup>R</sup>*). *SacB* gene encodes the *Bacillus subtilis* levansucrase enzyme. The enzyme catalyzes the hydrolysis of sucrose, generating products that are toxic for *E. coli*<sup>66</sup>.

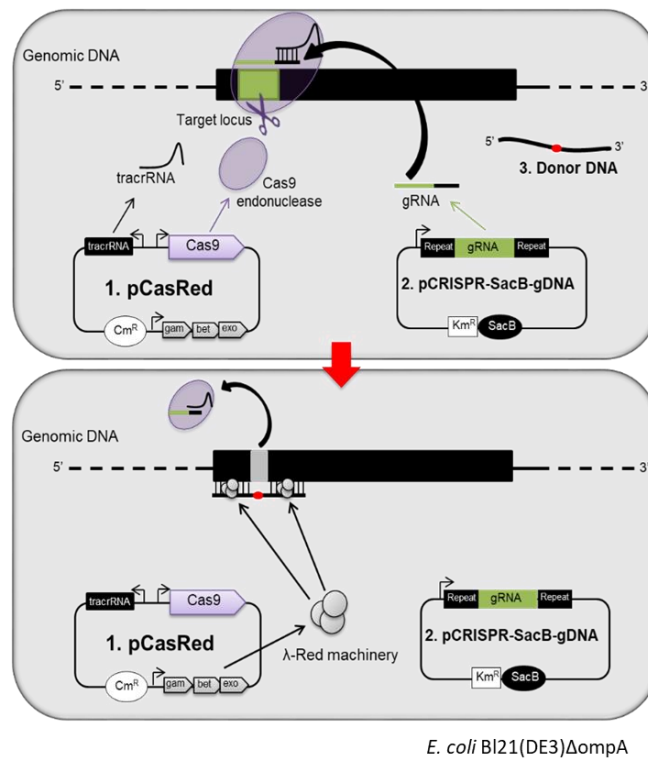


**Figure 4: Overview of CRISPR/Cas9 genome editing strategy in *Escherichia coli*** (from Zerbini et al., 2017). The strain to be mutagenized [*E. coli* BL21(DE3) $\Delta$ ompA] is first transformed with the pCasRed plasmid expressing the  $\lambda$  Red (*Exo*, *Beta*, *Gam*) machinery, the Cas9 endonuclease, and tracrRNA. Subsequently, the strain is co-transformed with pCRISPR-*SacB*-gDNA, and a synthetic, mutation-inducing oligonucleotide [donor DNA (dDNA)]. The pCRISPR-*SacB*-gDNA plasmid encodes the gRNA that specifies the site of cleavage and the endonuclease Cas9 recognizes the gRNA together with the tracrRNA, which anneals to gRNA forming a three-component complex. After the base pairing of gRNA to the target site, the Cas9 mediates the chromosomal DNA double strand break (upper panel). The double strand break is repaired by  $\lambda$  Red-mediated homologous recombination taking place between the extremities of the cleaved chromosomal DNA and the donor DNA (lower panel).

According to our protocol, the *E. coli* strain that has to be modified at a specific target locus is transformed with pCasRed plasmid. Subsequently, the strain is co-transformed with pCRISPR-*SacB*-gDNA and the donor DNA (dDNA). The Cas9 nuclease, guided by the gRNA, drives the cleavage of the genomic DNA at the target site, thus producing a double strand break (DSB). The DSB is repaired by  $\lambda$  Red-mediated homologous recombination taking place between the extremities of the cleaved chromosomal DNA and the donor DNA (Figure 4). This protocol was

fine-tuned by investigating how it was affected by 1) selection of gDNA, 2) length and concentration of dDNA, 3) extension of gene deletion.

#### *Selection of guide DNA*

gDNAs are usually selected among those 30 nucleotide sequences followed by an NGG (PAM) trinucleotide which in the target gene do not share homologies with other regions in the chromosome (to avoid off-target cleavage). Routine bioinformatics tools (BLAST) are generally used to identify such sequences. However, what has not been fully investigated is the robustness of bioinformatics in gDNA selection.

To establish the effectiveness of gDNAs, we created sets of pCRISPR-gDNA plasmids and we compared the transformation efficiencies of the recombinant plasmids with the efficiency of the “empty” pCRISPR vector. In particular, we selected three target genes, *ompF*, *lpp* and *fecA*, and we designed four sets of different gDNAs, two of them targeting different sites at the 5' and 3' regions of *ompF* gene, respectively, and the other two sets targeting *lpp* and *fecA* at different positions. Colonies were selected on LB plates supplemented with Cm and Km. While the “empty” pCRISPR vector routinely gave a transformation efficiency of  $0.5 - 2 \times 10^6$  CFUs/ $\mu$ g of plasmid DNA, most of pCRISPR-gDNA plasmids had transformation efficiencies in the range of  $0.5 - 2 \times 10^3$  CFUs/ $\mu$ g of plasmid DNA (Figure 5), indicating that the gDNA properly mediated DSBs. However, two out of the 20 pCRISPR-gDNA plasmids (pCRISPR-*ompF* 5'\_C and pCRISPR-*lpp*\_C) gave a transformation efficiency close to the one observed with the empty vector, suggesting these two gDNA inefficiently mediated Cas9 cleavage.

From these experiments, we concluded that in silico selection allows the identification of gDNAs, which in most cases drive the Cas9-mediated cleavage with high efficiency. However, approximately 10% of selected gDNAs did not cause bacterial killing. “Good and bad” gDNAs can easily be discriminated by colony counting after transformation with the by colony counting after transformation with the pCRISPR plasmids carrying the selected gDNAs. Therefore, before modifying any target gene we routinely run the colony testing and if transformation efficiencies higher than  $10^3$  CFUs/ $\mu$ g of plasmid DNA are obtained we change the gDNA sequence of the plasmid.

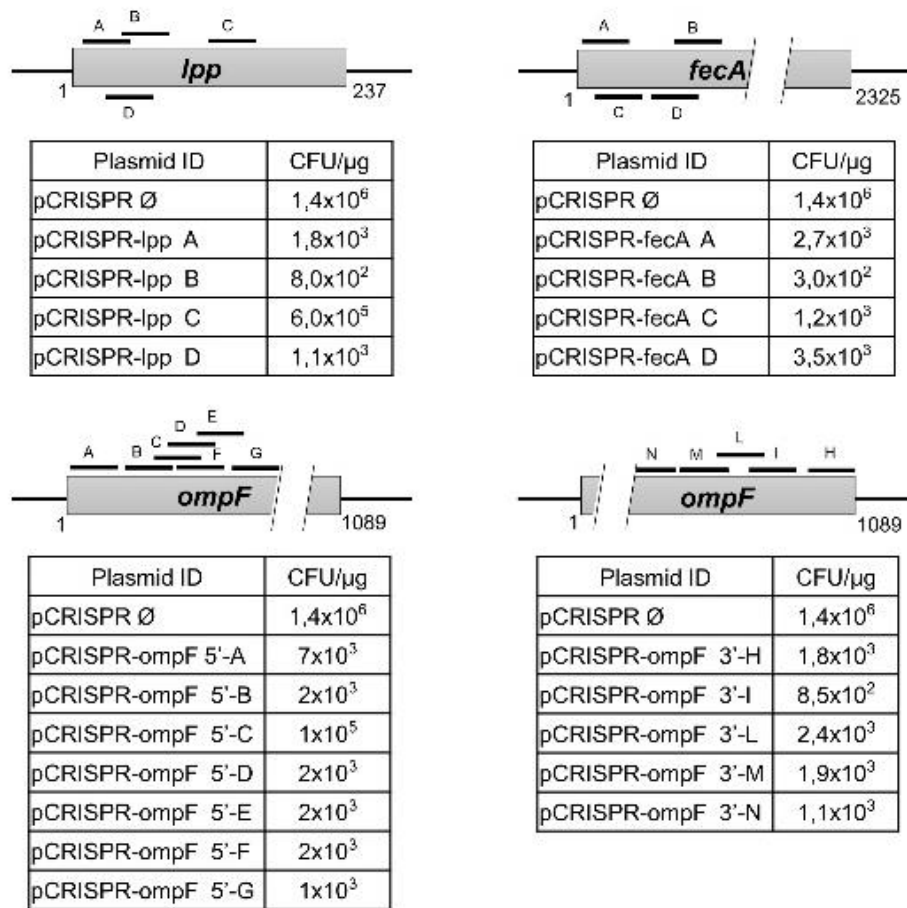


**Figure 5: Selection of gDNAs for mutation of *ompF*, *lpp* and *fecA* genes** (from Zerbini et al., 2017). The grey bars are a schematic drawing of the genes *lpp*, *fecA* and *ompF*, and the black lines labelled with letters indicate the positions where the gRNAs transcribed from their corresponding gDNAs hybridize within each gene. The tables report the transformation efficiencies (CFU/μg) of each pCRISPR-gDNA in BL21(DE3) $\Delta$ *ompA*.

#### Selection of the optimal conditions for gene knockout

To investigate the optimal condition for gene inactivation using the CRISPR/Cas9 protocol, four parameters were analyzed: length and concentration of the mutagenic dDNA, extent of gene deletion and type of donor DNA. The parameters were tested targeting four loci: the 5' end of the *ompF* gene the 3' end of the *ompF* gene, and the *fecA* and *lpp* genes. As a donor DNA, single stranded DNA (ssDNA) oligos annealing to the lagging strand (Lg-ss-dDNAs) or to the leading strand (Ld-ss-dDNA) and double strand DNA were used. The donor DNA were 120nt or 70nt long and were designed with homology arms of equal length upstream and downstream of the desired deletion. In addition, different concentrations, 1 and 10 μg, of donor DNA were used to test the gene knockout efficiency. All parameters were tested in

three different experiments and at least 20 colonies were analyzed to determine the mutation efficiency (Table 3).

**Table 3: Influence of type of donor DNA (dDNA) (Lg-ss-dDNAs, Ld-ss-dDNAs, ds-dDNA) length of dDNA, concentration of dDNA and size of deletion on mutagenesis efficiency at four chromosomal loci (from Zerbini et al., 2017).**

Target gene-pCRISPR-gDNA	Type of dDNA	dDNA ID	dDNA length (nt)	Mutation	dDNA quantity	Efficiency (%)-positive/total
ompF 5'-pCRISPR-ompF_5'G	Lg-ss	ompF 5'G-70-Δ30	70	Δ30	1	86% (19/22)
			70	Δ30	10	95% (40/42)
		ompF 5'G-70-Δ100	70	Δ100	10	5% (2/36)
			70	Δ500	10	0% (0/30)
		ompF 5'G-120-Δ30	120	Δ30	1	64% (40/62)
			120	Δ30	10	93% (76/82)
			120	Δ100	10	64% (20/31)
		ompF 5'G-120-Δ500	120	Δ500	10	47% (14/30)
	120		Δ1180	10	0% (0/20)	
	Ld-ss	ompF 5'G-70-Δ30 R	70	Δ30	10	20% (4/20)
		ompF 5'G-120-Δ30 R	120	Δ30	10	100% (10/10)
		ompF 5'G-120-Δ1089 R	120	Δ1180	10	0% (0/10)
	ds	ompF 5'G-120-Δ30 ds	120	Δ30	10	77% (20/26)
ompF 5'G-120-Δ500 ds		120	Δ500	10	50% (15/30)	
ompF 5'G-120-Δ1089 ds		120	Δ1180	10	26% (6/23)	
ompF 3'-pCRISPR-ompF_3'I	Lg-ss	ompF 3'I-70-Δ30	70	Δ30	10	79% (19/24)
		ompF 3'I-120-Δ30	120	Δ30	10	83%(25/30)
fecA-pCRISPR-fecA_B	Lg-ss	fecA B-70-Δ30	70	Δ30	10	43% (13/30)
		fecA B-120-Δ30	120	Δ30	10	77% (23/30)
		fecA B-120-Δ100	120	Δ100	10	20% (6/30)
		fecA B-120-Δ500	120	Δ500	10	13% (4/30)
		fecA B-120-Δ2325	120	Δ2325	10	0% (0/30)
	ds	fecA B-120-Δ2325 ds	120	Δ2325	10	14% (5/35)
lpp-pCRISPR-lpp_B	Lg-ss	lpp B-70-Δ30 R	70	Δ30	10	20% (4/20)
		lpp B-120-Δ30 R	120	Δ30	10	55% (11/20)
		lpp B-120-Δ237 R	120	Δ237	10	0%(0/16)
	Ld-ss	lpp B-70-Δ30	70	Δ30	10	90% (27/30)
		lpp B-120-Δ30	120	Δ30	10	73% (19/26)
		lpp B-120-Δ237	120	Δ237	10	0% (0/30)
	ds	lpp B-120-Δ30 ds	120	Δ30	10	82% (19/23)
		lpp B-120-Δ237 ds	120	Δ237	10	72% (18/25)

As far as ss-dDNA is concerned, both 70 and 120 base donor oligonucleotides (10 ug/ml) gave mutagenesis efficiency greater than 40% when 30 bp deletions were produced. However, for deletions longer than 30 bp, the 70 base ss-dDNA performed very poorly resulting in a mutation efficiency lower than 5%. The mutagenic efficiency was improved by extending the length of the oligonucleotide from 70 to 120 base ss-dDNA, allowing deletions around up to 500 nt with sufficiently good efficiencies. However, ss-dDNA performed very poorly for deletions bigger than 500 nt. Finally, the use of 120 bp long ds-dDNA, not only performed at least as well as ss-dDNA for short and medium deletions, but also allowed the full gene deletion of all the three target genes (*lpp*: 237 nt, *ompF*: 1180 nt and *fecA*: 2325 nt).

In summary, to achieve short deletions, 70 and 120 bp ss-dDNA oligonucleotides targeting either the lagging or leading strand perform similarly well with mutagenic efficiency between 50 and 100%. However, to achieve high frequency of long deletions 120 bp ds-dDNA is required.

#### *Validation of 30 bp gene deletions for mutant library production*

To validate the protocol described above, a list of 78 “dispensable” genes were selected. The design and selection of the 78 pCRISPR-*SacB*-gDNAs plasmids were performed according to the rules described above. The gDNAs were designed to target the genes next to their 5' ends of the open reading frame to avoid the expression of truncated proteins. Then, the gDNAs were cloned into pCRISPR-*SacB*-gDNAs plasmid and the efficacy of the gRNA to guide the Cas9 cleavage was tested by colony-counting. Since seven out of 78 gDNAs did not promote the cleavage of the target site, new gDNAs were designed and re-tested for these genes. After selecting optimal gDNAs, 70 nt long ss-dDNA oligonucleotides were designed for all target genes to delete around 30 bp and to introduce a premature stop codon in each gene. Of these 78 dDNAs, 46 targeted the leading strand and 32 the lagging strand. For each gene, its corresponding pCRISPR-*SacB* and its ss-dDNA was used to co-transform *E. coli* BL21(DE3) $\Delta$ *ompA*(pCasRed) strain, giving a transformation efficiency between 2 and  $5 \times 10^2$  CFUs/ug of plasmid DNA. Ten colonies were tested by PCR for each transformation to identify the percentage of those colonies carrying the 30 bp deletion on the target gene. Overall, 48 out of 78 genes selected were successfully mutated (Figure 6A). In particular, 20 out of 46 genes were successfully inactivated using the Lg-ss-dDNA, while, 28 out of 32 genes had the desired mutation using Ld-ss-gDNA.

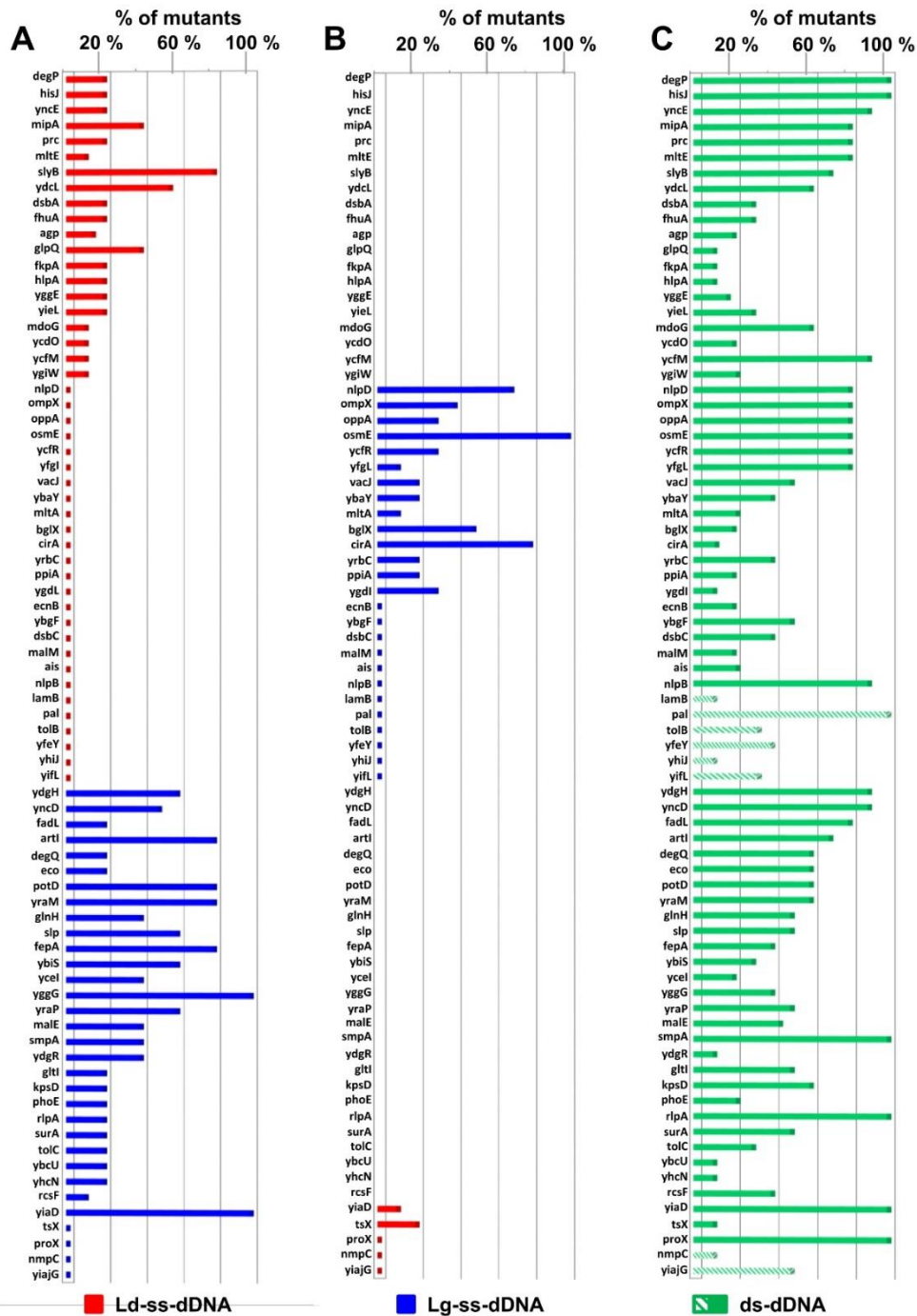


**Figure 6: Validation of 30 bp deletions on 78 genes** (from Zerbini et al., 2017). *E. coli* BL21(DE3) $\Delta$ ompA(pCasRed) or *E. coli* BL21(DE3)(pCasRed) were transformed with different mixtures of pCRISPR-*SacB*-gDNAs and 70-base dDNAs (either ssDNA or dsDNA) to mediate 30 bp deletion at one of the 78 selected gene loci (y axis). X axis indicates the percentage of mutants identified out of the total number of colonies analyzed. Bar height indicates the mutation frequency, while the presence of flat colored squares above gene names in each graph indicates that no mutants were identified out of ten colonies analyzed. Absence of bars or flat colored squares above gene names indicate that the gene mutation was not attempted for those specific genes in the experiment indicated in each bar graph. Red bars/squares indicate mutation experiments using Ld-ss-dDNAs; Blue bars/squares indicate mutation experiments using Lg-ss-dDNAs; Green bars/squares indicate mutation experiments using ds-dDNAs; bars with green downward diagonals indicate mutation experiments with ds-dDNAs in BL21(DE3)(pCasRed). **(A)** Bar graph representing mutation success rate using 46 Ld-ss-dDNAs (red bars/squares) and 32 Lg-ss-dDNAs (blue bars/squares). **(B)** Gene mutations that failed using the Ld-ss-dDNAs (26 genes out of 46) and the Lg-ss-dDNAs (4 genes out of 32) were re-attempted using ss-dDNAs targeting the opposite strands. **(C)** The bar graph represents the mutation success rate in BL21(DE3) $\Delta$ ompA(pCasRed) (green bars) and in BL21(DE3)(pCasRed) (green downward diagonal bars) using ds-dDNAs

To verify if the type of donor ss-DNA (leading vs lagging ss-DNA) has a role on the mutation frequency for those 30 genes that were not mutated, or at least not with a frequency equal or higher than 10% (1 colony out of 10), the mutagenic experiment was performed using the ss-dDNA targeting the opposite strand (Figure 6B). Regarding the 26 genes that failed to be mutated using the Ld-ss-dDNA, 14 were inactivated using Lg-ss-dDNA, while only 1 mutant was rescued using the Ld-ss-dDNA out of the 4 not obtained using the Lg-ss-dDNA.

Summarizing, 42 mutagenesis were obtained out of 58 targeted genes using Lg-ss-dDNA, corresponding to a success rate of 72%. On the other hand, targeting the leading strand with ss-dDNA the success rate was 43% corresponding to 22 inactivated genes out of 51 mutagenic experiments. Moreover, the average mutagenic frequency obtained with Ld-ss-dDNA was 10% compared with the 30% obtained using Lg-ss-dDNA.

Finally, we attempted the inactivation of the genes that failed to be mutated with ss-dDNA using as a donor 70 bp ds-dDNAs. As shown in Figure 6C, all genes were successfully mutated.

The conclusion of the extensive mutagenesis experiments carried out in BL21(DE3) strain is that our CRISPR/Cas9 gene editing protocol designed to delete 30-100 bp can reach a close to 100% efficiency and robustness when 70-120 bp ds-dDNA are used.

#### *Creation of multi-gene mutants by a stepwise approach*

Considering our goal to generate a multi-gene KO strain releasing proteome-minimized OMVs, we needed a genome editing tool not only efficient and robust, but that allowed to rapidly generate mutants in a stepwise modality. Therefore, we tested the performance of our genome editing protocol by testing the time needed to create the two-genes (*fecA* and *lpp*) mutant.

First, BL21(DE3) $\Delta ompA$ (pCasRed) strain was co-transformed with pCRISPR-*SacB-fecA\_B* plasmid and the ds-dDNA 120 base oligo *fecA\_B*-120- $\Delta$ 30. The day after 10 colonies were screened and 7 carried the expected mutation (70% mutagenesis efficiency) (Figure 7). One mutant clone was cultured overnight in LB media supplemented with Cm and 5% of sucrose. Under these conditions, the pCRISPR-*SacB-fecA\_B* was lost during overnight growth by virtue of the fact that the plasmid carries the *SacB* gene. This gene encodes an enzyme which catalyzes the production of high molecular weight fructose polymers, which are toxic for *E. coli*, and therefore, in order to survive, bacterial cells must lose pCRISPR-*SacB-fecA\_B*. Competent cells were made from the overnight culture of (BL21(DE3)  $\Delta ompA/\Delta fecA$ ) and co-

transformed with pCRISPR-*SacB-lpp\_B* plasmid and with ds-dDNA 120 base *lpp\_B*-120- $\Delta$ 240 oligo. Colonies screening revealed a 60% efficiency of *lpp* inactivation (Figure 7).

In conclusion, our pCRISPR/Cas9 genome editing protocol allows to generate a gene mutation every two days and in one week 2 to 3 genes can be inactivated from the same strain using the stepwise protocol described above.

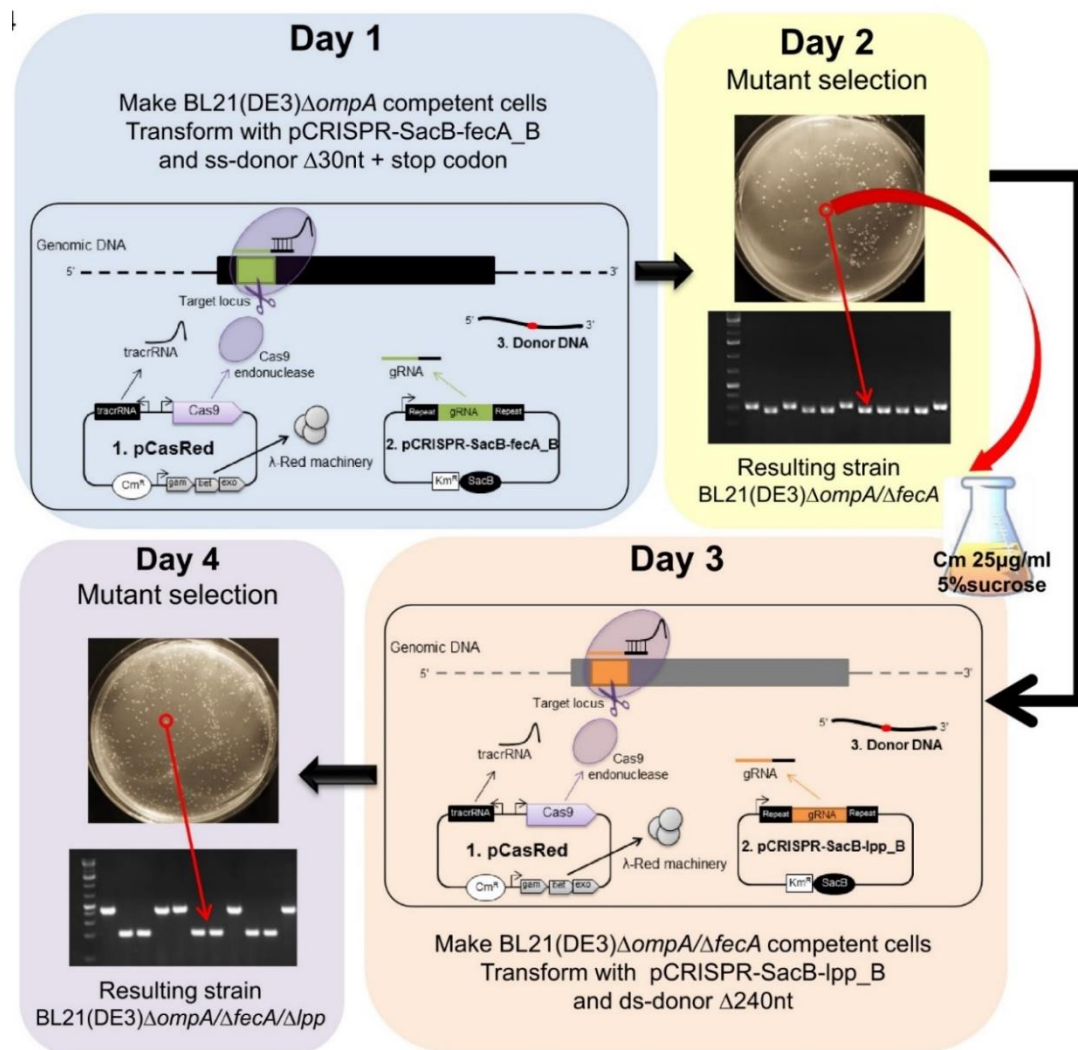


**Figure 7: Representation of the stepwise approach used to isolate strains carrying multiple mutations (from Zerbini et al., 2017).** **Day 1:** *E. coli* BL21(DE3) $\Delta$ *ompA*(pCasRed) was co-transformed with 1 µg/ml of pCRISPR-*SacB-fecA\_B* and 10 µg/ml of donor *fecA*-120- $\Delta$ 30nt and transformant colonies were selected on LB agar plates supplemented with Cm (25 µg/ml) and Km (50 µg/ml). **Day 2:** Ten colonies were randomly selected and screened by PCR using primers designed to generate DNA fragments from mutated colonies of 200 bp. PCR products were analyzed on 2% agarose gels. One mutant clone was subsequently inoculated into 5 ml of LB supplemented with 5% sucrose and 25 µg/ml Cm. **Day 3:** The overnight culture was used to prepare competent cells, which were subsequently co-transformed with 1 µg/ml of pCRISPR-*SacB-lpp\_B* and 10 µg of double strand donor DNA *lpp*-120- $\Delta$ 237. **Day 4:** Ten colonies were randomly selected and screened by PCR using primers designed to generate DNA fragments from mutated colonies of 400 bp. PCR products were analyzed on 2% agarose gels.

### Simultaneous gene deletions

Another approach that we tested has been the simultaneous inactivation of two genes. To this aim, we constructed pCRISPR plasmids encoding two gDNAs targeting two different loci of *E. coli* genome. Mimicking the same organization of the CRISPR arrays in bacteria, the two gDNAs were intercalated by the short repeated regions in the configuration “Repeat-gDNA1-Repeat-gDNA2-Repeat”. The pCRISPR-gDNA1-gDNA2 was used to transform the recipient strain with two ds-dDNAs, each designed to repair the target sites cleaved by the Cas9. The strategy was first tested to delete two stretches of 30 bp each at the 5' and 3' ends of the *ompF* gene. BL21(DE3) $\Delta$ *ompA*(pCasRed) was transformed with pCRISPR-*ompF*\_5'G-*ompF*\_3'I mixed with the two ds-dDNA *ompF*\_5'G-120- $\Delta$ 30 and *ompF*\_3'I-120- $\Delta$ 30. When colonies were analyzed by PCR screening, 12 out of 20 carried the deletion at both sites while only one carried a single mutation at the 5' end of the *ompF* gene (Figure 8A; Table 4.).

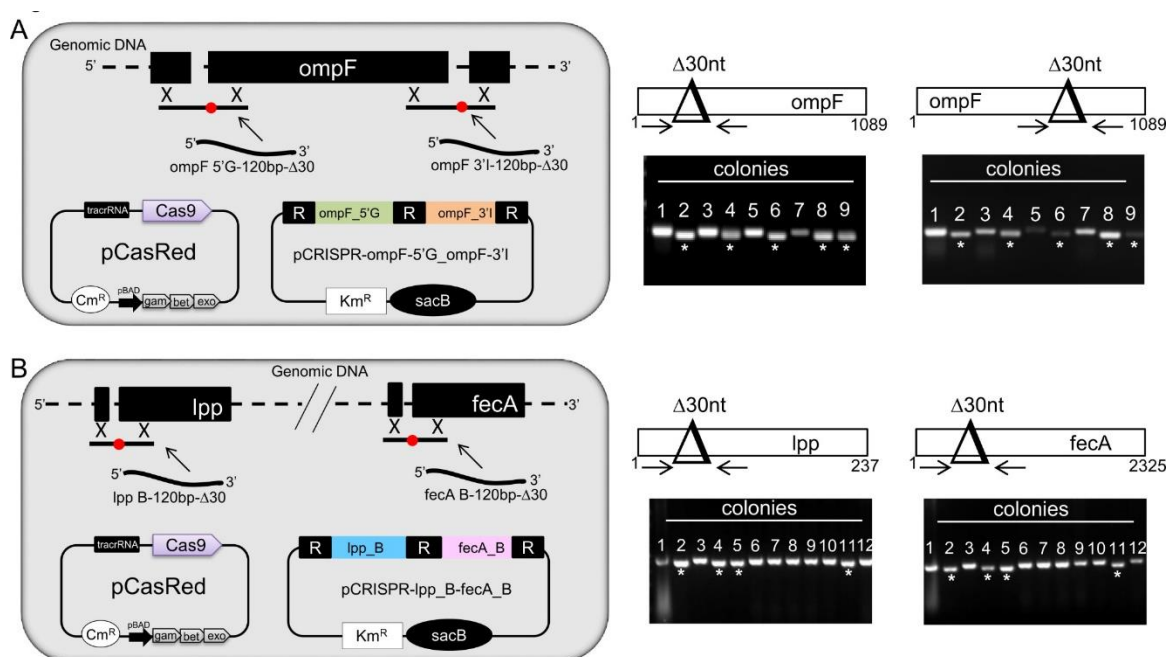


**Figure 8: CRISPR/Cas9-based protocol for simultaneous two-gene deletions** (from Zerbini et al., 2017). *E. coli* BL21(DE3) $\Delta$ *ompA*(pCasRed) was co-transformed with either 100 ng pCRISPR-*ompF*\_5'G-*ompF*\_3'I plasmid and the two dDNAs *ompF*\_5'G-120- $\Delta$ 30 and *ompF*\_3'I-120- $\Delta$ 30 (10  $\mu$ g each) (**A**) or with 100 ng pCRISPR-*lpp*\_B-*fecA*\_B and *lpp*\_B-120- $\Delta$ 30 and *fecA*\_B-120- $\Delta$ 30 dDNAs (10  $\mu$ g each). (**B**) Transformant colonies were selected on LB agar plates supplemented with 25  $\mu$ g/ml Cm and 50  $\mu$ g/ml Km. Colony PCR was carried out using two different couple of primers to screen each genomic locus (indicated at the bottom of each gel) on a randomly selected number of colonies and the PCR products separated on 2% agarose gels. Asterisks indicate those colonies in which deletion occurred at both gene loci.

**Table 4: Efficiency of simultaneous two-loci mutagenesis (*ompF* 5'/*ompF* 3' regions and *fecA/lpp* genes) using pCRISPR plasmids carrying repeat-gDNA<sub>1</sub>-repeat-gDNA<sub>2</sub>-repeat cassette (from Zerbini et al., 2017).**

pCRISPR-gDNA	dDNA ID	Mutation		
pCRISPR- <i>ompF</i> -5'G- <i>ompF</i> -3'I	<i>ompF</i> _5'G-120-Δ30	Δ30 <i>ompF</i> _5'	Δ30 <i>ompF</i> _3'	Δ30 <i>ompF</i> _5'/Δ30 <i>ompF</i> _3'
		10% (2/20)	Not tested	Not tested
pCRISPR- <i>ompF</i> -5'G- <i>ompF</i> -3'I	<i>ompF</i> _3'I-120-Δ30	Δ30 <i>ompF</i> _5'	Δ30 <i>ompF</i> _3'	Δ30 <i>ompF</i> _5'/Δ30 <i>ompF</i> _3'
		Not tested	0% (0/20)	Not tested
pCRISPR- <i>ompF</i> -5'G- <i>ompF</i> -3'I	<i>ompF</i> _5'G-120-Δ30+ <i>ompF</i> _3'I-120-Δ30	Δ30 <i>ompF</i> _5'	Δ30 <i>ompF</i> _3'	Δ30 <i>ompF</i> _5'/Δ30 <i>ompF</i> _3'
		5% (1/20)	0% (0/20)	57% (12/20)
pCRISPR- <i>lpp</i> _B- <i>fecA</i> _B	<i>lpp</i> B-120-Δ30+ <i>fecA</i> B-120-Δ30	Δ30 <i>lpp</i>	Δ30 <i>fecA</i>	Δ30 <i>lpp</i> /Δ30 <i>fecA</i>
		3% (1/29)	0% (0/29)	31% (9/29)

### 7.3 Construction of an *E. coli* strain releasing OMVs deprived of 58 endogenous proteins

With the data reported above, we have been able to demonstrate that our genome editing protocol is remarkably efficient and robust and allows to accumulate mutations at a pace of one mutation every two working days. Therefore, with this platform technology available we decided to initiate the construction of an *E. coli* strain which releases vesicles with a minimal number of endogenous proteins.

As illustrated in Section 4.2, mass spectrometry and bioinformatics analyses had led us to select 90 OMV protein-encoding genes as potential targets for genome editing.

For each of the 90 genes encoding the selected OMV proteins, gDNA were synthesized, cloned into a pCRISPR-*SacB*-gDNA and tested by colony counting to test their efficiency in guiding Cas9 chromosomal cutting. Subsequently, the cumulative inactivation of each gene was attempted following the random order reported in Figure 9. Once a gene was inactivated, before moving to the next deletion the mutant strain was characterized for its growth rate and OMVs production (Figure 9A). Our plan was in fact to eliminate those mutations that would have negatively affected growth or the OMV production.

Growth kinetics analysis was performed in flask. Each strain was inoculated in 50 mL LB-Miller and incubated at 30°C under vigorous shaking. The bacterial growth was followed over a period of 6 hours. At the end of the 6 hours culture, supernatant was separated by centrifugation, OMVs were then collected by ultracentrifugation (32,000 rpm for 2 h at 4°C) and the pellet was re-suspended in 100 μL PBS. The volumetric OMVs yield, expressed as total milligram protein per liter of bacterial culture, was calculated for each of the mutant *E. coli* strains (Figure 9A).

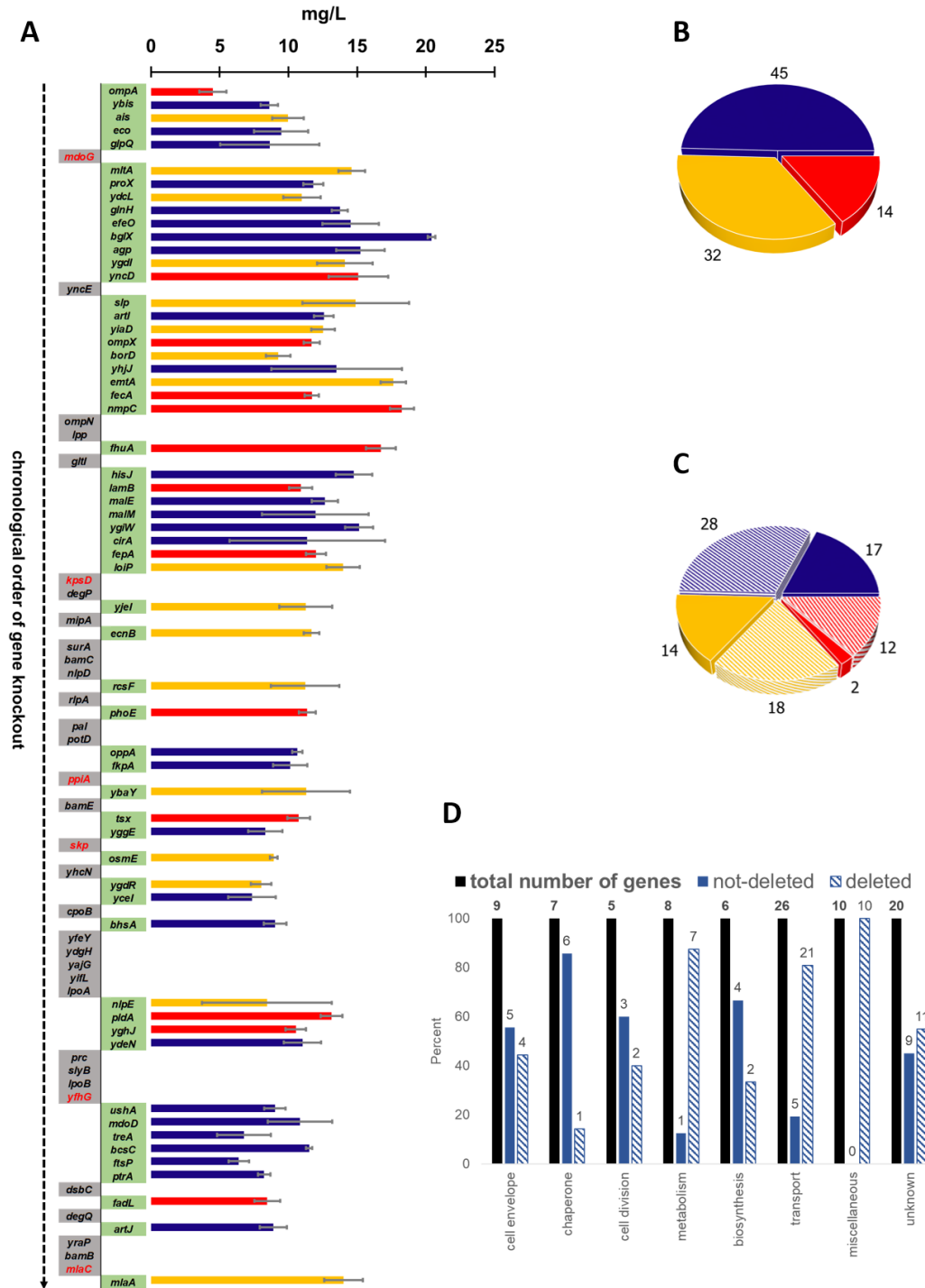


**Figure 9: Creation and characterization of *E. coli* BL21(DE3) $\Delta$ 58 strain. (A)** The chronological order of the 91 genes knock out. Underlined in grey are the genes that were not possible to delete, in green the genes that were inactivated. Each bar represent the volumetric OMVs yield (mg/l) of each strain performed in flask in a 50 ml volume at 30 °C for 6h, supernatant was separated by centrifugation, OMVs were then collected by ultracentrifugation (32,000 rpm for 2 hr at 4°C) and the pellets were re-suspended in 100  $\mu$ l PBS. **(B)** Classification of the 91 selected proteins for their compartmentalization. 45 proteins were identified as periplasmatic proteins (blue), 32 proteins were categorized as outer membrane  $\beta$  barrel proteins/porins (red). **(C)** Distribution of each protein category among the entire set of selected genes; those who we successfully deleted (filled pies) and the genes we could not delete (dashed pies). **(D)** The 91 selected proteins were classified in 8 function categories represented with the black bars, those who were successfully deleted are represented with dashed bars, while those we could not delete are represented with blue bars.

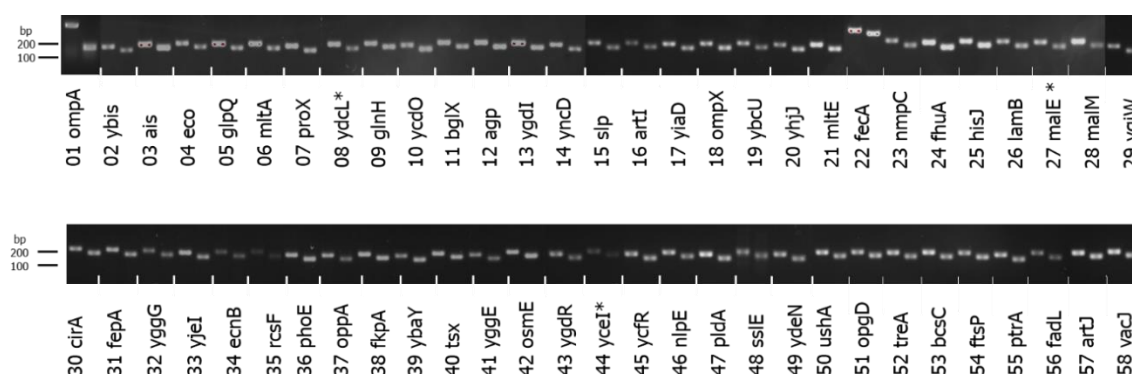
At the end, 57 OMV-associated genes out of 90 were successfully mutated, obtaining the *E. coli* strain named “**BL21(DE3)Δ58**”, since counting the *ompA* mutation, it features the inactivation of 58 genes encoding OMV localized proteins (Figure 9A). This strain produced significantly more OMVs than its progenitor *E. coli* BL21(DE3)Δ*ompA*.

Figure 9B groups the 90 proteins according to their cellular compartmentalization. As illustrated in the Figure 9B, 45 proteins belong to the periplasmic space (PP), 31 proteins are outer membrane lipoprotein (OM-LP) and 15 proteins are integral membrane protein (OM-BP/P). Interestingly, almost 90% of the 15 OM-BP/P proteins were successfully eliminated in BL21(DE3)Δ58 while the compatibility of the simultaneous elimination of the selected PP and OM-LP proteins dropped to about 55-60% (Figure 9C). Not surprisingly, most of the proteins whose function was associated to transport and metabolism could be eliminated while the simultaneous inactivation of proteins involved in envelope structure, metabolism and biosynthesis was less permissible (Figure 9D).

The correctness of the deletions created in each of the 58 genes of *E. coli* BL21(DE3)Δ58 was verified in two ways.

First, specific primer pairs were designed upstream and downstream from the deleted regions to amplify approx. 200 bp DNA fragments from the chromosomal DNA of *E. coli* BL21(DE3)Δ58. The same primers on *E. coli* BL21(DE3)Δ*ompA* DNA as a template should generate fragments 30 bp longer and such difference could be appreciated on a 2% agarose gel (Figure 10).

Second, the genome of *E. coli* BL21(DE3)Δ58 was fully sequenced and the sequence analysis confirmed the deletions in each of the 58 genes.



**Figure 10: Agarose gel showing PCR amplified fragments of all 58 genes mutated in *E. coli* BL21(DE3)Δ58.** The images show the difference in size (30 nucleotides) comparing the PCR products obtained using DNA template either from *E. coli* BL21(DE3)Δ*ompA* (left lane of the designated gene) or the *E. coli* BL21(DE3)Δ58 strain created in this study (right lane of the designated gene).

We finally verified whether the gene deletions resulted in the disappearance of the corresponding proteins from OMVs. To this aim, OMVs from *E. coli* BL21(DE3) $\Delta$ 58 and from its progenitor *E. coli* BL21(DE3) $\Delta$ ompA were separated by 2D-electrophoresis and the protein maps of the two proteomes were compared using bioinformatics tools. A substantial reduction of protein spots was clearly visible when the 2D maps were compared (Figure 11A-B). Interestingly, our previous characterization of progenitor OMVs by 2DE/mass spectrometry had led to the identification of several proteins including 42 out of the 57 proteins encoded by the deleted genes. All the spots corresponding to these 42 proteins were not present in the 2D map of OMVs from *E. coli* BL21(DE3) $\Delta$ 58 (Figure 11C).

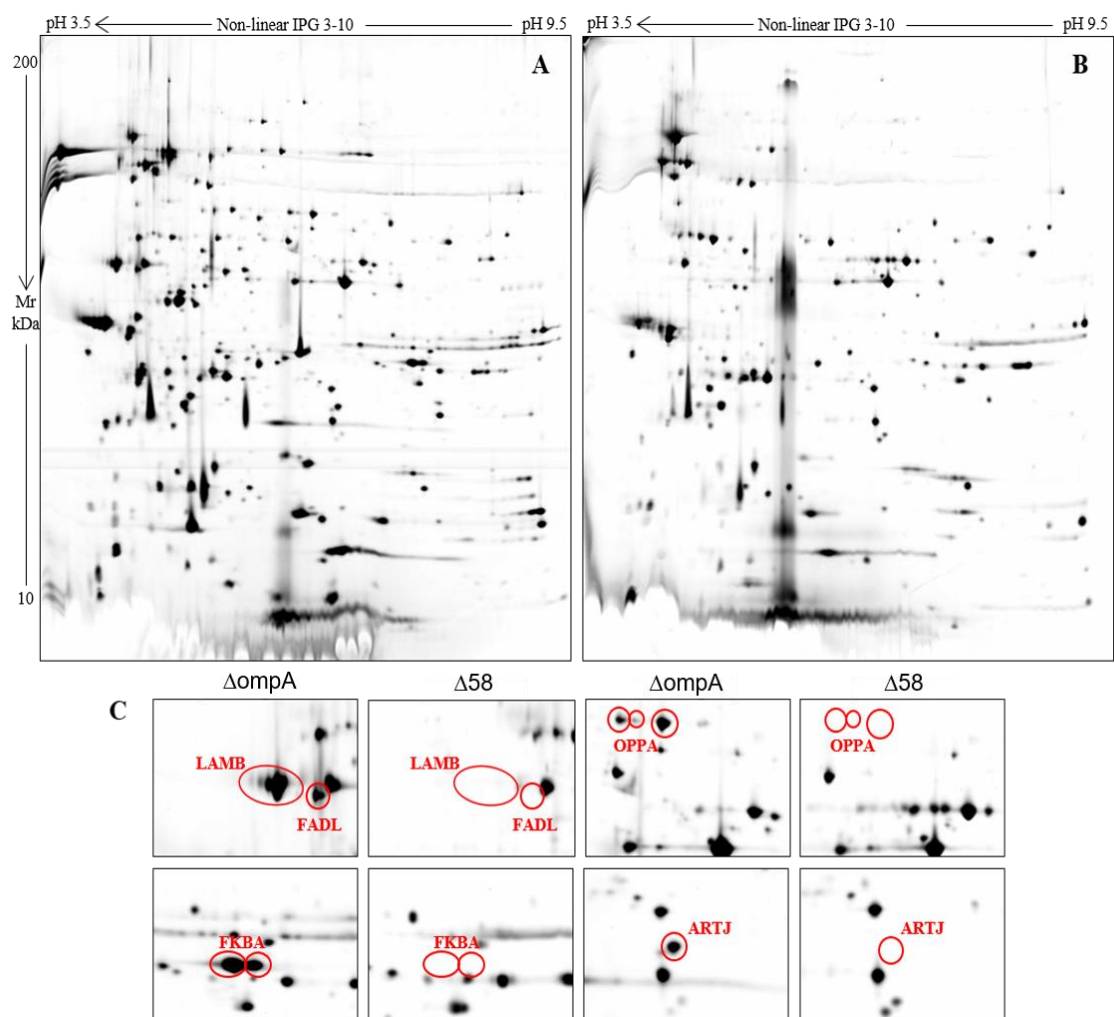


**Figure 11: Silver stained 2DE gels of OMVs from *E. coli* BL21(DE3) $\Delta$ ompA (A) and  $\Delta$ 58 (B) strains. (C) Zoomed areas of 2DE gels Red circles visualize significant qualitative differences detected in *E. coli* BL21(DE3) $\Delta$ ompA (spots encircled in red) and not in *E. coli* BL21(DE3) $\Delta$ 58 (empty red circles). Four examples of proteins are shown: Maltoporin (LAMB), Periplasmic oligopeptide-binding protein (OPPA), FKBP-type peptidyl-prolyl cis-trans isomerase (FKBA), and ABC transporter arginine-binding protein 1 (ARTJ).**

#### 7.4 Attenuation of LPS reactivity in *E. coli* BL21(DE3) $\Delta$ 58

One of the main concern regarding OMVs as an adjuvant platform is their reactivity mediated by LPS<sup>67</sup>. LPS is composed of three main structural domains: O-specific polysaccharide, the core polysaccharide and Lipid A. This latter component is naturally present in *E. coli* in a hexa-acylated form and it is recognized by TLR4, a receptor that belongs to the PRR family. Lipid A binding to TLR4/MD2 complex results in dimerization of the receptor, thus leading to the activation of an intracellular signaling which ultimately results in the production of inflammatory cytokines.

The Lipid A interaction to TLR4/MD2 occurs via its acyl moieties<sup>15</sup> and it has been shown that Lipid A carrying a lower number of acyl chains has a reduced TLR4 agonistic activity<sup>39</sup>. The production of penta-acylated Lipid A in *E. coli* can be achieved by inactivating two genes of the lipid A biosynthetic pathway (*msbB* and *pagP*), which encode two acyltransferases enzymes (Figure 12).

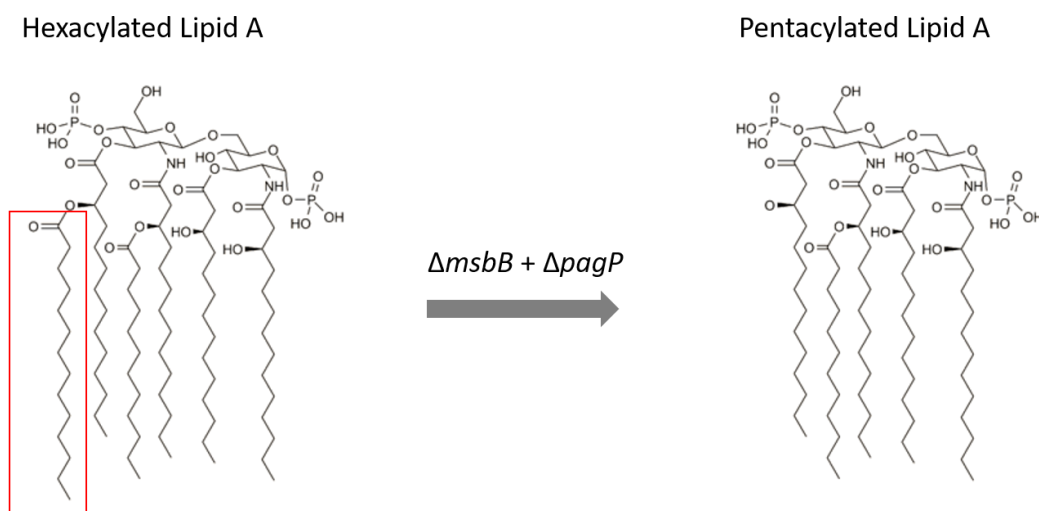


**Figure 12: Schematic overview of hexacylated and pentacylated LPS.** Lipid A component of LPS is usually present in highly-reactogenic hexacylated conformation. Mutations in *msbB* and *pagP* genes should result in low-reactogenic pentacylated conformation.

Therefore, *E. coli* BL21(DE3) $\Delta$ 58 strain was further modified by introducing two additional mutations in the *msbB* and *pagP* genes by using CRISPR/Cas9 editing genome protocol. The new derivative was named *E. coli* BL21(DE3) $\Delta$ 60.

The hTLR4 agonistic activities of OMVs from *E. coli* BL21(DE3) $\Delta ompA$ , *E. coli* BL21(DE3) $\Delta$ 58 and *E. coli* BL21(DE3) $\Delta$ 60 using a hTLR4 activation assay based on HEK-Blue™ hTLR4 cells.

These cells, upon stimulation of their surface-exposed hTLR4 with a proper TLR4 agonist, activate the expression of a reporter gene encoding an alkaline phosphatase, whose activity is proportional to the potency of the TLR4 agonist. As shown in Figure 13, *E. coli* BL21(DE3) $\Delta$ 60-derived OMVs had a hTLR4 agonistic activity almost one order of magnitude lower than the agonistic activity of OMVs from *E. coli* BL21(DE3) $\Delta$ 58 and from their progenitor *E. coli* BL21(DE3) $\Delta$ ompA.

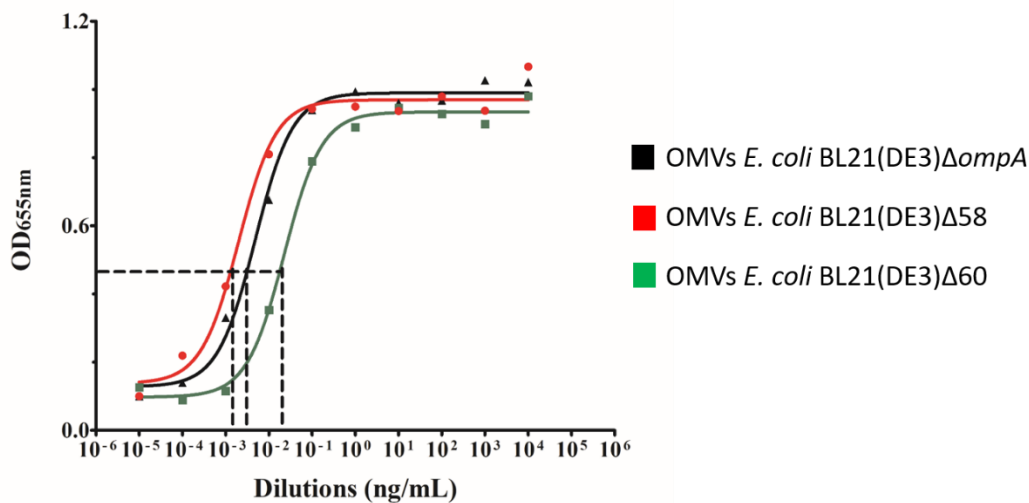


**Figure 13: Human Toll Like Receptor 4 (hTLR4) activation analysis by OMVs from *E. coli* BL21(DE3) $\Delta$ ompA, *E. coli* BL21(DE3) $\Delta$ 58 and *E. coli* BL21(DE3) $\Delta$ 60.** LPS reactivity was tested through hTLR4 activation assay based on a colorimetric reaction to detect SEAP activity. OMVs were isolated from different strains and were initially diluted to a concentration of 10,000 ng/ml and then serial dilutions of 10-fold were prepared. OMVs from *E. coli* BL21(DE3) $\Delta$ ompA (blue), *E. coli* BL21(DE3) $\Delta$ 58 (red) and *E. coli* BL21(DE3) $\Delta$ 60 (dark green) were compared. For each curve, dashed lines indicate the potencies of OMVs as agonists of hTLR4.

### 7.5 *E. coli* BL21(DE3) $\Delta$ 58 and $\Delta$ 60 strains releasing proteome-minimized OMVs show a significant increase in OMV production capacity

To be exploited as a vaccine platform, OMV production has to be scaled up to volumes compatible with industrial needs. Therefore, the kinetic growth and the OMVs production of *E. coli* BL21(DE3) $\Delta$ ompA(pET\_empty), *E. coli* BL21(DE3) $\Delta$ 58(pET\_empty) and *E. coli* BL21(DE3) $\Delta$ 60(pET\_empty) were tested in the bioreactor. Growth was carried out in a 2 l fermentation unit in LB supplemented with ampicillin (100 ug/ml, final concentration), 15 g/l glycerol, 0.25 g/l MgSO<sub>4</sub>. The temperature was kept at 30°C until OD<sub>600</sub> = 0.5, and then the temperature was shifted down to 25°C. The growth parameters were: pH 6.8 ( $\pm$ 0.2), dO<sub>2</sub> > 30% and rpm between 280-500. As shown in Figure 11, all three strains had similar growth kinetics. By contrast, *E. coli* BL21(DE3) $\Delta$ 58 showed an 11.2 fold increase in OMV production

compared to its progenitor, while *E. coli* BL21(DE3) $\Delta$ 60 OMV production was 7-fold higher than *E. coli* BL21(DE3) $\Delta$ ompA (Figure 14).

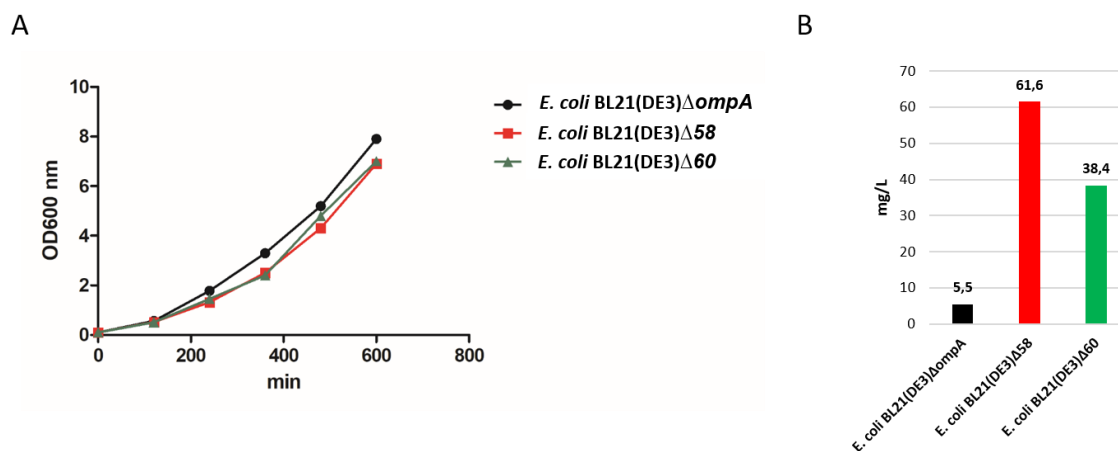


**Figure 14: Analysis of growth kinetic and OMV productivity for *E. coli* BL21(DE3) $\Delta$ ompA, *E. coli* BL21(DE3) $\Delta$ 58 and *E. coli* BL21(DE3) $\Delta$ 60 in the bioreactor. (A)** The growth of *E. coli* BL21(DE3) $\Delta$ ompA (red), *E. coli* BL21(DE3) $\Delta$ 58 (red) and *E. coli* BL21(DE3) $\Delta$ 60 (green) in bioreactor (2 l, 30 °C and then 25 °C, for 10h) was followed at regular intervals. **(B)** The bar graph shows the volumetric yield of total protein content in OMVs purified from *E. coli* BL21(DE3) $\Delta$ ompA (black), *E. coli* BL21(DE3) $\Delta$ 58 (red) and grown *E. coli* BL21(DE3) $\Delta$ 60 (green) a bioreactor.

## 7.6 Expression of heterologous antigens in the strains releasing proteome-minimized OMVs

Next, the expression of heterologous antigens and their delivery to the OMV compartment was analyzed in *E. coli* BL21(DE3) $\Delta$ 58 and *E. coli* BL21(DE3) $\Delta$ 60.

First, we investigated the surface delivery of heterologous antigens by flow cytometry. Three antigens were tested. Two of them were constituted by the *Neisseria* lipoprotein Fhbp fused to (i) the 13 aa peptide LEEKKGNVVTDH belonging to EGFRvIII (EGFRvIIIpep), a mutated form of the human epidermal growth factor receptor (EGFR)<sup>68</sup>, and (ii) the D8-FAT1 epitope IQVEATDKDLGPNGHVTVSIVTDTD expressed in human colon cancer<sup>69</sup>. The third antigen was D8-FAT1 fused to the *S. aureus* protein FhuD2.

The plasmids encoding the fusion proteins were used to transform *E. coli* BL21(DE3) $\Delta$ ompA and *E. coli* BL21(DE3) $\Delta$ 58. The strains were grown in flask at 37°C to mid-log phase and antigen expression was induced for 2 hours by the addition of 0.1 mM IPTG. Cells were collected, incubated with the specific antibodies and subsequently with secondary Alexa Fluor<sup>®</sup>488 anti-rabbit total IgGs antibodies. Finally, cells were fixed with 2% formaldehyde and analyzed by flow cytometry.

Interesting, *E. coli* BL21(DE3) $\Delta$ 58 strain shows a higher capacity to express all three selected heterologous antigens on its surface with respect to its progenitor (Figure 15).

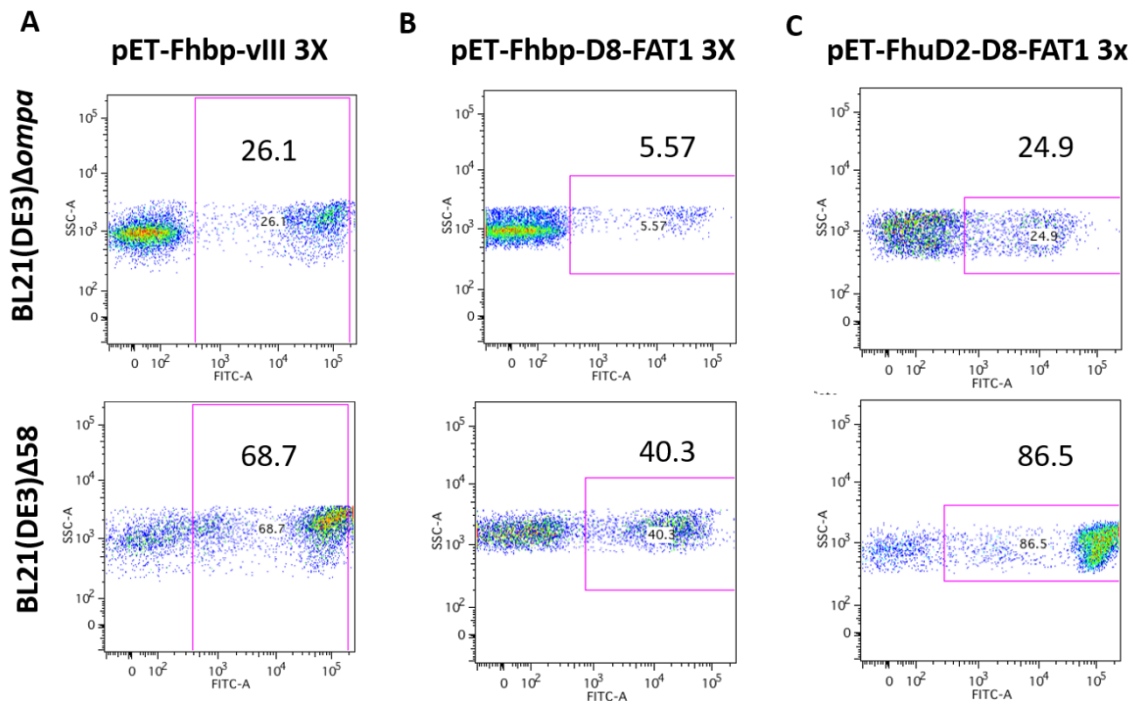


**Figure 15: Heterologous antigens are exposed on the surface of *E. coli* BL21(DE3) $\Delta$ ompA and *E. coli* BL21(DE3) $\Delta$ 58.** Flow cytometry analysis. Bacterial cells from BL21(DE3) $\Delta$ ompA and *E. coli* BL21(DE3) $\Delta$ 58 were transformed with (A) pET-Fhbp-vIII 3x (B) pET-Fhbp-D8-FAT1 3x and (C) pET-fhuD2-D8-FAT1 3x. The strains were stained with rabbit  $\alpha$ -specific epitope antibodies. Signal was detected using Alexa Fluor<sup>®</sup> 488  $\alpha$ -rabbit IgGs antibodies. As a control, cell were stained with Alexa Fluor<sup>®</sup> 488  $\alpha$ -rabbit IgGs antibodies only (not shown).

Next, the OMV compartmentalization of the following five antigens was investigated: SpA, LukE and FhuD2 from *S. aureus*, and the two fusion proteins FhuD2-D8-FAT1 3x and FhuD2-OVA 3x.

*E. coli* BL21(DE3) $\Delta$ 58 and *E. coli* BL21(DE3) $\Delta$ 60 were transformed with the antigen-encoding plasmids and the engineered strains were analyzed for their capacity to release OMVs carrying the corresponding recombinant antigen. The strains were grown in flask at 30°C to mid-log phase and antigen expression was induced for 4 hours by the addition of 0.1 mM IPTG. Finally, the cell cultures were harvested by centrifugation and OMVs were purified from the filtered supernatant. The expression of the heterologous antigens in the purified OMVs was analyzed by SDS-PAGE. All the 5 antigens were efficiently compartmentalized in the OMVs with an expression level ranging from 5% (in the case of LukE) to >20% (FhuD2-OVA 3x) (Figure 16).

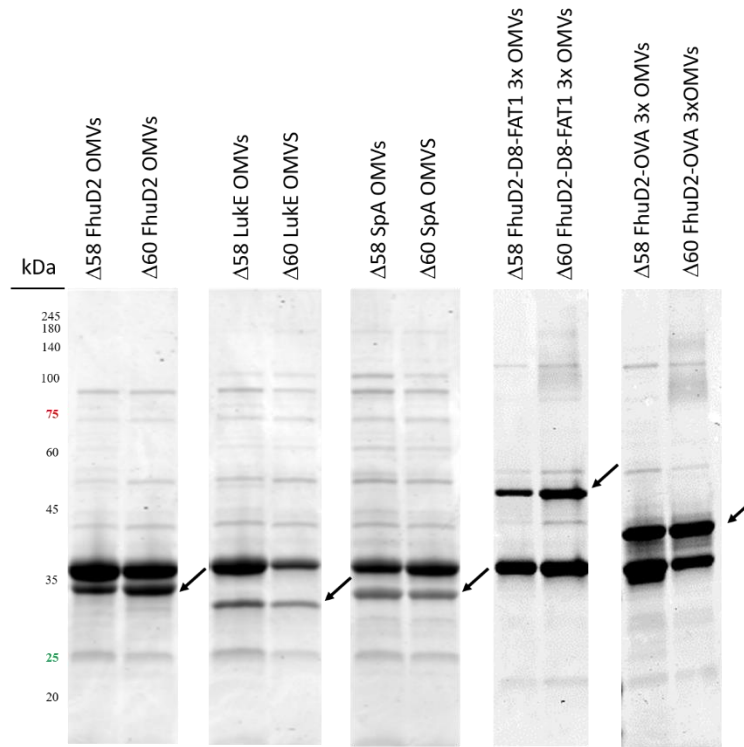


**Figure 16: Efficient expression of heterologous antigens in OMVs derived from *E. coli* BL21(DE3)Δ58 and Δ60 strains.** SDS-PAGE analysis of 5 µg of OMVs purified from *E. coli* BL21(DE3)Δ58 and Δ60 pET-Lpp-fhuD2 (fhuD2 OMVs), pET-Lpp-Luke (Luke OMVs), pET-Lpp-SpA (SpA OMVs), pET-Lpp-FhuD2-D8-FAT1 3x (FhuD2-D8-FAT1 3x OMVs) and pET FhuD2-OVA 3x (FhuD2-OVA 3x OMVs). Heterologous antigens are indicated with an arrow.

## 7.7 Immunogenicity of engineered OMVs from *E. coli* BL21(DE3)Δ58 and *E. coli* BL21(DE3)Δ60 strains

We next asked the question whether OMVs from engineered *E. coli* BL21(DE3)Δ58 and *E. coli* BL21(DE3)Δ60 could induce antigen-specific immune responses in experimental animals. To this aim, CD1 outbred mice were immunized i.p. three times at days 0, 14 and 28 with 5 µg of SpA-OMVs, Luke-OMVs, FhuD2-OMVs and D8-FAT1-OMVs derived either from *E. coli* BL21(DE3)Δ58 or *E. coli* BL21(DE3)Δ560. After two weeks from the third immunization, sera were collected and antigen-specific antibodies titers were analyzed by ELISA. To this aim, plates were coated with 200 ng/well of antigen (FhuD2, Luke and SpA were purified from *E. coli* while D8-FAT1 was chemically synthesized (see Materials and Methods)) and incubated with different dilutions of the corresponding sera. Antibody binding was finally revealed using goat anti-mouse IgG conjugated to alkaline phosphatase. As shown in Figure 17, all engineered OMVs elicited good antigen-specific antibody titers and no significant difference was observed between OMVs derived from BL21(DE3)Δ58 and *E. coli* BL21(DE3)Δ60.

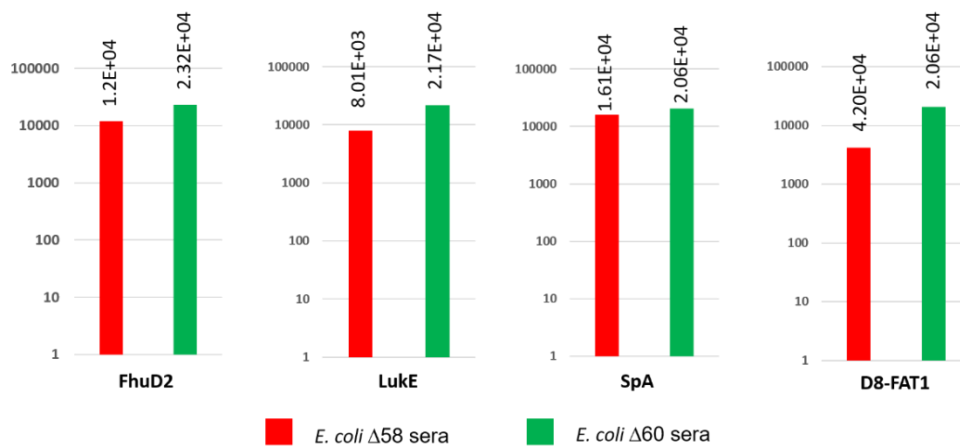


**Figure 17: Antigen-specific IgG titers from mice sera elicited by immunization with OMVs from *E. coli* BL21(DE3)Δ58 and Δ60 strains expressing either FhuD2, LukE, SpA or D8-FAT1.** Bar graphs represent total IgG titers for sera obtained from mice immunized with OMVs purified from *E. coli* BL21(DE3)Δ58 (red) and *E. coli* BL21(DE3)Δ60 (green) expressing either FhuD2, LukE, SpA or FhuD2-D8-FAT1 3x, calculated as dilutions corresponding to an absorbance of 2.

Next, we analyzed if OMVs engineered OMVs FhuD2-OVA 3x could induce epitope-specific CD8+ T cell response. To this aim, we immunized C57BL/6 mice with 5 μg of FhuD2-OVA 3x OMVs derived either from *E. coli* BL21(DE3)Δ58 or *E. coli* BL21(DE3)Δ60.

Mice were vaccinated two times on day 0 and day 7. At day 12 spleen was collected and splenocytes were stimulated with 2mg/ml of OVA peptide or as a control with an irrelevant peptide. INFγ producing CD8+ T cells analyzed by flow cytometry and OVA-specific CD8 T cell population was calculated as a percentage of the whole CD8 T cells. As shown in Figure 18, both FhuD2-OVA OMVs from *E. coli* BL21(DE3)Δ58 and *E. coli* BL21(DE3)Δ60 were shown to stimulate OVA-specific CD8+ T cell. Interestingly, stimulation with OMVs from *E. coli* BL21(DE3)Δ60 appeared to be particularly pronounced, the OVA-specific IFN-γ+ CD8+ T cells representing more than 1% of total CD8+ T cell population.

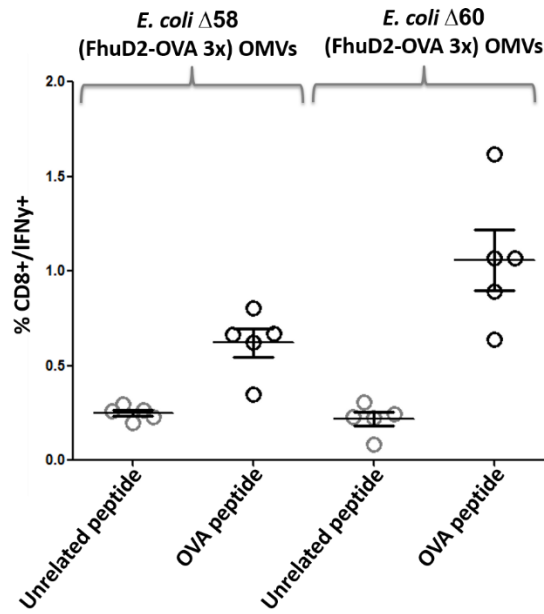


**Figure 18: OMVs derived from *E. coli* BL21(DE3)Δ58 or Δ60(pET-Lpp-FhuD2 OVA 3x) elicit specific CD8 T cell response**  
 Splenocytes from mice treated with OMVs derive from *E. coli* BL21(DE3)Δ58(pET-Lpp-fhuD2 OVA 3x) or *E. coli* BL21(DE3)Δ60(pET-Lpp-fhuD2 OVA 3x) were in vitro stimulated with OVA peptide or with an unrelated peptide mix as a control. The release of IFN-γ by CD8 T cells able to recognize the OVA was determined by flow cytometry.

## 8 Discussion

OMVs are being extensively and successfully utilized in preclinical and clinical settings for prophylactic vaccination against infectious diseases. Their unique adjuvanticity, which directs the immune responses toward a Th1 profile, and the ease with which they can be manipulated and purified have attracted the attention of several academic and industrial groups. There are a number of bacterial OMV-based vaccines that are already available for human use. However, for full-blown exploitation of OMVs as a vaccine platform, a few aspects require optimization. They include: 1) development of universal and efficient strategies for OMV engineering, 2) reduction of OMV endogenous proteins to avoid potential interference in the elicitation of proper immune responses against heterologous antigens, and 3) the modulation of the potent OMV adjuvanticity to mitigate the risk of unwanted reactogenic responses.

The aim of this work was twofold. First, to apply synthetic biology to create a novel *E. coli* derivative releasing proteome-minimized OMVs featuring high immunogenicity and low reactogenicity. Second, to demonstrate the usefulness of such strain as a platform for infectious disease and cancer vaccines.

We believe that this study has generated a number of relevant results.

First, thanks to the combination of in-silico analysis and 2D Electrophoresis coupled to Mass Spectrometry we have been able to define a detailed map of the proteins present in the OMVs from *E. coli* BL21(DE3)/ $\Delta ompA$ . Importantly, many of the proteins have been defined not only in qualitative but also in quantitative terms, and we now have good information on which are the most and least abundant proteins of the OMV proteome. Our study can be useful to better understand the biogenesis and functions of *E. coli* OMVs. Furthermore, such information can be exploited in the development of new diagnostic, drug and vaccine targets.

A second important contribution of this work has been the development of a genome editing protocol based on the cutting edge CRISPR/Cas9 technology. The exploitation of CRISPR/Cas9 protocols for prokaryotic genome editing had been published by a number of groups<sup>61,70,71</sup>. However, information on the broad efficiency and the robustness of the technology was missing. To fill this gap, we systematically tested different parameters including, the sequence of the gRNA, the length and concentration of the donor DNA, and use of ss-dDNA and ds-dDNA to define the most effective conditions for gene knock out in *E. coli*.

As far as the the selection of the gDNA is concerned, any sequence next to the PAM trinucleotide should represent a good target site for the Cas9 cleavage. However, we found that 10% of the designed gDNA did not promote Cas9 DSB with high specificity. Although we still do not have a plausible explanation for this phenomenon (we looked for the presence of sequences forming internal stem-loop structures, or partially complementary to other chromosomal regions not carrying the NGG trinucleotides) our work provides a simple and effective protocol to discriminate “good” from “bad” gDNA, which simply involved a colony counting step after transformation with gRNA-encoding plasmid.

Court and co-workers demonstrated that “λ Red recombineering” in *E. coli* is more efficient in promoting mutagenesis event if performed with Lg-ss-dDNAs than Ld-ss-dDNAs. Like other authors<sup>62,71</sup>, we confirmed the superiority of the Lg-ss-dDNA even when “λ Red recombineering” is combined with CRISPR/Cas9, a situation where the mechanism that leads to the introduction of the site-specific mutation must be coupled to the mechanism of double-stranded DNA repair. However, we showed that ds-DNA clearly outperforms ssDNA as donor DNA, and therefore our work offers an important guideline for optimal gene inactivation.

One of the main features of our protocol is the speed with which genes can be inactivated: multiple mutations can be introduced at a pace of one mutation every two days. This was possible thanks to the strategy we used to remove the high copy number plasmid pCRISPR-*SacB*-gDNA after each mutagenesis step. Different strategies have been used to remove high copy number plasmids, a classical one being the use of a temperature sensitive origin of replication<sup>70</sup>. We exploited the toxic effect of the *SacB* gene when *E. coli* is grown in media containing high concentrations of sucrose. This strategy, which was previously reported by others groups for chromosomal gene knock-in/knock-out experiments<sup>72,66</sup>, was previously suggested for plasmid curing by others<sup>73</sup>, and we unequivocally validated its effectiveness in this work.

To allow the simultaneous inactivation of two different loci, the pCRISPR-*SacB* plasmid can be modified to carry two different gDNA sequences. We mimicked the conformation of CRISPR array using the configuration repeat-gDNA1-repeat-gDNA2-repeat achieving high frequency of mutation. Previously, Yu Jiang performed the simultaneous knockout of two different genes but when using synthetic ssDNA donor they were not able to recover double mutant colonies<sup>71</sup>.

A third important message of this work is that, by using the CRISPR/Cas9 genome editing protocol developed in our laboratory, we demonstrated for the first time that a considerable

proportion of proteins belonging to the OMV proteome can be eliminated without impairing cell viability and growth rate of the mutated strains, at least under laboratory conditions. In particular, we managed to create a strain, we named *E. coli* BL21(DE3) $\Delta$ 58, carrying the deletion of 58 genes coding for OMV proteins.

From a scientific standpoint, this information paves the way to a better understanding of function and interaction of proteins belonging to the periplasmic and outer membrane compartments of *E. coli*. In our attempt to simultaneously inactivate genes encoding OMV-associated proteins (proteins belonging to the “dispensable” family according to the Keio collection), we attempted the deletion of 91 dispensable genes and we found that the deletion of 33 of them was not compatible with the presence of the other 58 mutations. The information about the incompatibility of certain combinations of mutations could shed light on the biological role of the mutated proteins, particularly of those with unknown function. It is in fact conceivable to hypothesize that if certain mutations are incompatible, the corresponding inactivated proteins might share vital functions the cell tries to secure through functional redundancy.

From a translational viewpoint, *E. coli* BL21(DE3) $\Delta$ 58 strain has a number of interesting features.

First of all, we discovered that the removal of the 58 OMV proteins led to the release of an impressive amount of OMVs. When grown in the bioreactor, we consistently obtained more than 60 mg/l of OMVs (protein content), a quantity approximately 11-fold higher than the yield obtained from the progenitor. The mutation of *vacJ*, the last gene mutation added to the strain, appeared to substantially contribute to the hyper-vesiculating phenotype, even though most of the intermediate mutant strains also showed a propensity to release high quantities of OMVs. *VacJ* is part of the *VacJ/Yrb* ABC phospholipid transporter whose inactivation has been proposed to increase vesiculation through a novel mechanism<sup>74</sup>. Second, the inactivation of the 58 endogenous OMV proteins does not impair the capacity of *E. coli* BL21(DE3) $\Delta$ 58 strain to accumulate heterologous antigens in the vesicular compartment. Indeed, we tested the expression of a number of antigens and we found that all of them could be efficiently delivered to the OMVs, their expression ranged from approximately 5% to over 20% of total OMV proteins. Interestingly, when the heterologous proteins were expressed as lipoproteins, *E. coli* BL21(DE3) $\Delta$ 58 was found to efficiently delivered such proteins to the cell surface with very high efficiency. The mechanisms which

make *E. coli* BL21(DE3) $\Delta$ 58 a better strain for surface lipoprotein exposition with respect to its *E. coli* BL21(DE3)/ $\Delta$ ompA progenitor remain to be fully elucidated.

Third, we showed that OMVs from *E. coli* BL21(DE3)/ $\Delta$ 58 engineered with a number of heterologous antigens elicit excellent immune responses in experimental animal models. This is true for antibody responses but also for cell-mediated immunity. In particular, we showed that OMVs decorated with a fusion protein carrying the OVA CD8<sup>+</sup> T cell epitope, induced OVA-specific CD8 T cell population, supporting the data that OMVs elicit potent cell mediated responses<sup>75</sup>.

Fourth, our data showed that the potential reactogenicity of OMVs from *E. coli* BL21(DE3)/ $\Delta$ 58 could be modulated by altering the LPS biosynthetic pathway. LPS is the main OMV structure that affect safety, in fact LPS naturally results in excessive secretion of pro-inflammatory cytokines in organisms<sup>67</sup>. We created a new detoxified OMV strain by inactivating in *E. coli* BL21(DE3)/ $\Delta$ 58 two genes involved in the acylation of Lipid A (*msbB* and *pagP*), *E. coli* BL21(DE3)/ $\Delta$ 60, which released OMVs featuring a reduced TLR4 agonistic activity, expanding OMVs safety in vaccine platforms.

Such strain maintained the same properties as *E. coli* BL21(DE3)/ $\Delta$ 58 in terms of heterologous antigen expression in OMVs and immunogenicity, thus representing a promising candidate for the development of novel vaccines having both of low-toxicity and high-immunogenicity.

In conclusion, we believe that our work represents an important step-forward for the optimization of OMVs as vaccine platform. Our future plans are to confirm the usefulness of *E. coli* BL21(DE3)/ $\Delta$ 58 and *E. coli* BL21(DE3)/ $\Delta$ 60 strains in preclinical models, with the ultimate goal to reach the clinics for cancer applications in a few years from now (2021-2022).

## 9 Materials and methods

### 9.1 Bioinformatics

The follow proteome analysis tools were used to identify bioinformatically the “surfactome” of *E. coli*: Proteome Analyst, SOSUI-GramN and PSORTb version 3.0.2. The “Keio collection”<sup>76</sup>, was used as a basis to evaluate both the biological functions and the non-essentiality of the selected genes listed in (Results Table 1). To properly select the gDNA and to avoid off-target effects of Cas9 we use the tool BLAST as previously described<sup>77</sup>.

### 9.2 Construction of plasmids

The pCasRed plasmid carries a chloramphenicol resistance gene (CmR) and encodes the Cas9 nuclease, the  $\lambda$  Red (Exo, Beta, Gam) cassette and the tracrRNA. The *Cas9* gene and the tracrRNA coding sequence are under the control of constitutive promoters while the  $\lambda$  Red gene cassette is transcribed using an arabinose-inducible promoter. The pCas9 plasmid (ADDGENE #42876)<sup>64</sup> was used as template for the construction of pCasRed plasmid and the  $\lambda$  Red cassette was PCR amplified from pKOBEG plasmid<sup>65</sup> and was cloned into pCas9 plasmid using the polymerase incomplete primer extension (PIPE) cloning method<sup>78</sup> as described previously<sup>77</sup>.

The pCRISPR-*SacB* plasmid, derived from pCRISPR plasmid (ADDGENE #42875)<sup>64</sup>, where a kanamycin resistance gene (KmR) is fused to the *SacB* gene encoding the *Bacillus subtilis* levansucrase, carries the synthetic DNA fragment (gDNA) coding for the guide RNA necessary to drive the Cas9-dependent double stranded break at the desired site of the bacterial genome. The construction of the pCRISPR-*SacB* plasmid was carried out by the PIPE method in two steps as described priviusly<sup>77</sup>. First, the kanamycin resistance cassette of pCRISPR plasmid was replaced by a “cat-sac cassette” containing the chloramphenicol acetyltransferase gene, along with the *SacB* gene, from pKM154 plasmid (ADDGENE #13035)<sup>79</sup>.

Plasmids expressing the gRNAs, were constructed by phosphorylation and annealing of oligonucleotides (gDNAs) (Zerbini et al. 2017), followed by ligation into pCRISPR (or pCRISPR-*SacB*) digested with BsaI (New England BioLabs). The resulting constructs were used to transform *E. coli* DH5 $\alpha$  strain (Invitrogen) and the plasmids prepared by QIAprep Spin Miniprep Kit, Qiagen (QIAGEN kit) were analyzed by DNA sequencing.

Plasmids expressing heterologous antigens were made by PIPE method and were previously cloned in our laboratory in the pET21b+ plasmid.

The construction of pET-Nm-FHbp and pET-Nm-FHbp-vIII 3x plasmids expressing the *Neisseria meningitidis* FHbp and FHbp fused to three repeated copies of EGFRvIII peptide was cloned as previously described<sup>44</sup>.

To cloning the constructs expressing the *S. aureus* antigens Luke, FhuD2 and SpA the coding sequences of the antigens were chemically synthesized (Genart-Invitrogen) and PCR amplified using the primers listed below. The PCR products were inserted into pET-Lpp plasmid, pET21 derivatives carrying the sequence encoding the leader peptide for secretion of *E. coli* Lpp using the PIPE cloning method. Plasmids were linearized using the primers couples: Lpp-R-plasmid/nohisflag. The DNA mixtures were then used to transform *E. coli* HK100 competent cells and the correctness of the cloning was verified by sequence analysis.

**Table 5: Primers for antigens fusion to the Lpp Leader sequence and cloning into pET21B**

Nohisflag V-f	TAACATCACCATCACCATCAGATTACAAAGA
Lpp-R-plasmid	GCTGGAGCAACCTGCCAGCAGAG
Lpp-FhuD2-f1	CTGCTGGCAGGTTGCGGGAACCAAGGTGAAAAAATAACAAAG
FhuD2-r1	GTGATGGTGTATGTTATTTTGCAGCTTTAATTAATTTTTCTTTAAATCTTTAC
Lpp-SpA-f1	CTGCTGGCAGGTTGCGCACAGCATGATGAAGCCAAAAA
SpA-r1	GTGATGGTGTATGTTATTTAGGTGCCTGTGCGTCGTT
Lpp-Luke-f1	CTGCTGGCAGGTTGCAACTAATAATTGAAAATATTGGTGTATGGTGC
Luke-r1	GTGATGGTGTATGTTAATTATGTCCTTTCACCTTAATTTTCGTGTGTTTTCCA

For the construction of pET-Fhbp-D8-FAT1 3x and pET-FhuD2-D8-FAT1-3x, three copies of D8-FAT1 were fused to the C-terminus of the *S. aureus* Fhbp or FhuD2 lipoprotein. D8-FAT1 minigene was constructed by assembling six complementary oligonucleotides (listed below). The assembled DNA fragment was amplified with primers F-FATFH/R-FATFH F-FATFhuD2/R-FATFhuD2 (Appendix) to make its extremities complementary to linearized pET21-Fhbp and pET21-FhuD2. pET21-Fhbp and pET21-fhuD2 were linearized using primers fhbp-F/fhbp-R and fhuD2-F/ fhuD2-R, respectively. The DNA mixtures were then used to transform *E. coli* HK100 competent cells and the correctness of the cloning was verified by sequence analysis.

**Table 6: Oligos used to assemble the synthetic D8-FAT1 minigene**

F1-FAT	ATCAAGTGGGAAGCGACTGACAAAGATCTGGGCCCGAATGGCCAT
R1-FAT	ATCTGTATCCGTAACGATTGAATAAGTTACATGGCCATTCGGGGCC
F2-FAT	ACGGATACAGATATCCAGGTAGAGGCAACCGATAAAGATTTAGGTCCC
R2-FAT	GGTATCCGTTACGATACTATATGTGACGTGGCCATTGGGACCTAAATC
F3-FAT	GTAACGGATACCGACATTCAGGTGGAAGCTACCGATAAAGACCTGGGTCCG
R3-FAT	ATCTGTATCGGTAACAATAGAATACGTCACGTGACCATTCGGACCCAGGTC

**Table 7: Primers to insert D8-FAT1 minigene gene into pET21-Fhbp and pET21-FhuD2**

F-FATFH	CTTGCCGCAAGCAAATTCAGTGGAAGCG
R-FATFH	GTGATGGTGATGGTGATGTTAATCTGTATCGGTAAC
fHbp-F	TAACATCACCATCACCATCACGATTACAAAGA
fHbpFL-R	TTATTGCTTGGCGGCAAGGC
fhuD2-F	CATCACCATCACCATCACGATTACA
fhuD2-R	TTTTGCAGCTTTAATTAATTTTC
F-FATFhuD2	TAATTAAGCTGCAAAAATTCAGTGGAAGCGACTGA
R-FATFhuD2	GATGGTGATGGTGATGTCAATCTGTATCGGTAACATAG

To clone pET-FhuD2-OVA 3x, three copies of OVA epitopes fused with a linker of glycine-glycine was synthesized and purchased from GeneArt® Gene Synthesis (LifeTechnologies). pET-FhuD2 was linearized using Nohisflag and FhuD2-Rev primers, OVA minigene (CAGCTGGAAAGCATTATTAAC TTTGAAAACTGACCGAAGGTGGTCAGCTGGAAAGCATTATTAAC TTTGAAAACTGACCGAAGGTGGTCAGCTGGAAAGCATCATCAACTTCGAAAACTGACCGAA) was amplified by PCR using primers couple OVAPSP-F/OVAPSP-R. Finally, PCR products were mixed together and used to transform *E. coli* HK100 competent cells.

**Table 8: Primers to insert OVA mini gene into pET21-FhuD2**

OVAPSP-F	TAATTAAGCTGCAAAACAGCTGGAAAGCATTATTAAC TTTGAAAAAC
OVAPSP-R	TGGTGATGGTGATGTTATTCGGTCAGTTTTTCGAAGTTGATGATGCTTTC
FhuD2-Rev	TTTTGCAGCTTTAATTAATTTTCTTTTAAATCTTTACGC
Nohisflag	TAACATCACCATCACCATCACGATTACAAAGA

### 9.3 Bacterial strains and culture conditions

*E. coli* DH5 $\alpha$  strain was routinely grown in LB broth (SIGMA) at 37 °C and used for cloning experiments. *E. coli* BL21(DE3) $\Delta ompA$  strain and its mutant derivatives strains were grown in

LB broth at 37 or 30 °C when required, and were employed for genome editing experiments and antigen expression analysis. Stock preparations of strains were prepared in LB + 20% glycerol and stored at -80 °C. Each bacterial manipulation was started using an overnight culture from a frozen/glycerol stock. When required, kanamycin and chloramphenicol or ampicillin were added to final concentrations of 50 µg/ml, 25 µg/ml or 100 µg/ml, respectively.

For fermentation processes, an EZ control bioreactor (Applikon) was used and condition were set as follows: volume 2 l; temperature 30°C until OD600 0.5, then growth continued at 25°C; pH 6.8 (±0.2), dO<sub>2</sub> > 30%; rpm 280-500 rpm; at OD600 1.0 feed was performed by adding 1 ml ampicillin (100 mg/ml), 15 g/l glycerol, 0.25 g/l MgSO<sub>4</sub>.

#### 9.4 Competent cell preparation

Chemically competent cells were used to prepare *E. coli* BL21(DE3) $\Delta$ *ompA*/pCasRed and to transform pET plasmid encoding heterologous antigen in *E. coli* BL21(DE3) $\Delta$ *ompA*, *E. coli* BL21(DE3) $\Delta$ 58 and *E. coli* BL21(DE3) $\Delta$ 60. Cells from glycerol stock were inoculated in 5 mL LB and incubated overnight (O/N) at 37°. The pre-cultures were diluted to an optical density at 600nm (OD<sub>600nm</sub>) of 0.1 in 50 ml LB and incubated at 37°C until an OD<sub>600nm</sub> of 0.4-0.6 was reached. The cell cultures were harvested through centrifugation at 4 °C, 2.500 x g for 20 minutes, resuspended in 5 ml of ice-cold, sterile 100 mM MgCl<sub>2</sub> and kept in ice for 30 minutes. Subsequently, cells were centrifuged at 4 °C, 2.500 x g for 20 minutes, resuspended in 1 mL of ice-cold, sterile 100 mM CaCl<sub>2</sub> in 15% glycerol and aliquoted for storage at -80°C. 100 ng of purified pCasRed plasmid or pET plasmid containing the gene of interest were mixed with 50 µl of chemically competent cells and kept in ice for 30 minutes. Subsequently, cells were transferred to a thermoblock and heat-shocked at 42°C for 45 seconds and placed on ice for another 2 minutes. 950 µl of LB was added to the reaction and incubated for 1h at 37°. For the selection step, cells were plated on LB-agar plates, containing 25 µg/ml chloramphenicol or 100 µg/ml, and incubated overnight at 37°C.

Mutagenesis experiments were performed using electro competent cell. *E. coli* BL21(DE3) $\Delta$ *ompA* and its mutant derivative strains carrying pCasRed plasmid were used. To prepare electro competent cells a 5 ml overnight culture (LB medium) inoculated from a single colony of *E. coli* BL21(DE3) $\Delta$ *ompA*(pCasRed) or its mutant derivative strains obtained from an LB-agar plate was grown LB medium with 25 µg/ml chloramphenicol at 37 °C under vigorous

shaking. The overnight culture was diluted to an OD<sub>600</sub> of 0.1 and grown at 37 °C under shaking (200 r.p.m.) to an OD<sub>600</sub> of 0.2 and then l-arabinose was added to a final concentration of 0.2% for λ Red induction. After induction, the culture was grown to an OD<sub>600</sub> of 0.7 and then cells were washed, aliquoted and stored at -80°C.

### 9.5 Gene knockout using CRISPR-Cas9

For mutagenesis experiments oligonucleotides (donor DNA or dDNAs) (see Zerbini et al. 2017) were HPLC purified grade. The dDNAs were designed to delete a region ranging from 30 (Δ30) to 2325 (Δ2325) nucleotides from target genes, removing the protospacer and PAM regions adding an in-frame stop codon downstream the deleted region. For the leading and lagging strand design, the oligonucleotides annealing to the 3' > 5' strand moving clockwise from OriC up to ter were Ls-ss-dDNAs, while oligonucleotides annealing to the same strand but moving counterclockwise from OriC up to ter were Lg-ss-dDNAs. The opposite was true for the oligonucleotides annealing to the 5' > 3' strand moving clockwise from OriC up to ter and for those annealing to the same strand moving counterclockwise from OriC to ter. The ds-dDNAs were generated by annealing 10 µg of both forward and reverse oligonucleotides in a total volume of 20 µl at 95 °C for 5 min and allowing the reaction mixture to cool down at room temperature. The annealing reaction was verified by loading 500 ng of each single stranded oligonucleotides and 1 µg of total DNA in the annealing reaction and by visualizing the bands using ATLAS ClearSight DNA Stain (BIOATLAS). For CRISPR/Cas9-mediated gene knockouts 50 µl of competent cells were electroporated using 1 mm Gene Pulser cuvette (Bio-Rad) at 1.8 kV with 100 ng of pCRISPR-gDNA or pCRISPR-SacB-gDNA plasmid and either 1 or 10 µg of oligonucleotide donor DNA. As control, 100 ng of an empty pCRISPR plasmid was used. Cells were then immediately re-suspended in 1 ml of LB medium and allowed to recover at 30 °C for 3 h under agitation before being plated on LB agar with 25 µg/ml chloramphenicol and 50 µg/ml kanamycin and incubated at 37 °C overnight. Mutants were screened by colony PCR using GoTaq master mix (Promega-M7123). Individual colonies were picked and directly resuspended in PCR reaction mix and DNA amplification was carried out according to the standard cycling GoTaq protocol.

### 9.6 OMV purification and SDS-PAGE

*E. coli* BL21(DE3)ΔompA strain and its mutant derivative strains were transformed with pET empty plasmid or encoding the genes of interest. Recombinant clones were grown at 30°C and 180 rpm in LB medium (starting OD<sub>600</sub> = 0.05) and, when the cultures reached an OD<sub>600</sub>

value of 0.5, protein expression was induced by addition of 0.1 mM IPTG (Sigma-Aldrich). After 4 hours, culture supernatants were separated from living bacterial cells by a centrifugation step at 6,000 x g for 15 minutes followed by a filtration through a 0.22 µm pore size filter (Millipore) or for larger volume Tangential Flow Filtration was performed using a Hollow Fiber cartridge UFB-500-C-3MA (General Electrics). Supernatants were then subjected to high-speed centrifugation (200,000 x g for 2 hours) and pellets containing the OMVs were finally re-suspended in sterile 1X PBS. OMVs amounts were estimated by measuring protein concentration using DC protein assay (Bio-Rad). 10 µg of OMVs (protein content) were resuspended in sodium dodecyl sulfate-polyacrylamide gel electrophoresis (SDS-PAGE) Laemmli buffer and heated at 100°C for 10'. Proteins were separated using Any kD™ Criterion™ TGX Stain-Free™ Protein Gel (BioRad) in TrisGlycine buffer (BioRad). Finally proteins were revealed by Coomassie Blue staining.

#### 9.7 Purification of recombinant *S. aureus* antigens

Recombinant *S. aureus* antigens were purified using the TEV protease purification strategy<sup>80</sup>. Briefly, the synthetic genes coding for SpA, LukE and FhuD2 were fused at their 5' to the sequence coding for a His 6 -tag and the TEV cleavage site. The constructs were cloned in a pET15 plasmid downstream of a T7 inducible promoter and expressed in *E. coli* BL21(DE3) strain. Bacterial biomass (5 g wet weight) was resuspended in 50 ml buffer A (50 mM NaH<sub>2</sub>PO<sub>4</sub>, 300 mM NaCl, pH 8.0) in the presence of a protease inhibitor (0.2 mM PMSF), sonicated thoroughly at 4°C and the total cell lysate was finally centrifuged (15.000 x g, 30 min, 4°C). The supernatant was filtered (0.22 µm) and applied to Ni-affinity chromatography (IMAC) using an ÄKTA purifier System (GE) and a 5 ml HiTrap IMAC column (GE) monitoring absorbance at 280 nm. Protein binding and column washing was performed at concentrations of 20 mM and 50 mM imidazole, respectively. Bound proteins were elute using a linear gradient by increasing buffer B (50 mM NaH<sub>2</sub>PO<sub>4</sub>, 300 mM NaCl, 500 mM imidazole, pH 8.0) from 10% to 100% over 6 CV. Pooled fractions containing the His-tagged recombinant protein was dialysed against buffer A at 4°C and subsequently digested with TEV protease (1 mg per 100 mg protein) in the presence of 5 mM β-mercaptoethanol. TEV-digested protein pool was applied to Ni-affinity chromatography and the flow-through, containing the untagged recombinant protein, was applied to a final polishing step by size-exclusion chromatography using a HiLoad 16/600 Superdex 75 pg column.

## 9.8 In vitro assay for human Toll Like Receptor 4 activity analysis

The experiment was conducted to detect the level of activation of the human Toll Like Receptor 4 (hTLR4) using HEK-Blue™ hTLR4 Cells and QUANTI-Blue (InvivoGen) as substrate according to the manufacturer's protocol.

OMVs isolated from *E. coli* BL21(DE3) $\Delta$ *ompA*, *E. coli* BL21(DE3) $\Delta$ 58 and *E. coli* BL21(DE3) $\Delta$ 60, transformed with pET plasmid, were tested for hTLR4 activation and as positive control LPS was used. OMVs and LPS were initially diluted to a concentration of 10,000 ng/ml and then serial dilutions of 10-fold were performed. 20  $\mu$ l of each dilution were added in the dedicated well on a 96-well plate and, subsequently, 180  $\mu$ l of HEK-Blue™ hTLR4 Cells (~140,000 cells/ml) were added to each well and incubated overnight at 37°C. The following day, 20  $\mu$ l of supernatant from SEAP-expressing HEK-Blue™ hTLR4 Cells were added to 180  $\mu$ l QUANTI-Blue™ in a new 96-well plate and incubated at 37°C for 30 min. The absorbance of the colorimetric reaction was measured at 655 nm using an Infinite M200PRO plate reader (TECAN).

## 9.9 Flow cytometry on bacteria

*E. coli* BL21(DE3) $\Delta$ *ompA* or *E. coli* BL21(DE3) $\Delta$ 58 strain transformed with either pET-Fhpb-vIII 3x, pET-Fhpb-hFAT1 or pET-FhuD2-hFAT1 3x and were grown at 37°C and 180 rpm in LB medium (starting OD600 = 0.05) and, when the cultures reached an OD600 value of 0.5, protein expression was induced by addition of 0.1 mM IPTG (Sigma-Aldrich). After induction, a volume corresponding to OD=1 was collected from each culture and centrifuge at 14,000 rpm 10'. Pellet was resuspended in 1ml PBS/BSA 1% and further diluted 1:50 in PBS/BSA 1%. 50  $\mu$ l/well were put in 96 well plate. 50  $\mu$ l of 2x solution of rabbit  $\alpha$ -vIII or  $\alpha$ -hFAT1 antibodies respectively (final concentration is 8  $\mu$ g/ml) in PBS/BSA 1% were added in selected wells and cell incubated for 1h at 4°C. Cells were then washed 2 times with 100-200  $\mu$ l/well of PBS/BSA 1% and centrifuged centrifuge for 10' at 3500 rpm and 4°C. 100  $\mu$ l/well of Alexa Fluor®488  $\alpha$ -rabbit IgGs (Thermo Fisher Scientific) diluted 1:200 (final concentration is 10  $\mu$ g/ml) in PBS/BSA1% were added in selected wells and incubated for 1h at 4°C in the dark. Cells were then washed 2 times with 100-200  $\mu$ l/well of PBS/BSA 1% and centrifuged centrifuge for 10' at 3,500 rpm and 4°C. Cells were fixed with 100  $\mu$ l PBS/Formaldehyde 2% for 15' at room temperature. Cells were then washed 2 times with 100-200  $\mu$ l/well of PBS and centrifuged centrifuge for 10' at 3,500 rpm and 4°C. Cells were finally resuspended cells in 200  $\mu$ l of PBS

and stored at 4 °C in the dark or acquired to the Flow cytometry. Data were analyzed using FlowJo v10.1.

## 9.10 Animal studies

Mice were monitored twice per day to evaluate early signs of pain and distress, such as respiration rate, posture, and loss of weight (more than 20%) according to humane endpoints. Animals showing such conditions were anesthetized and subsequently sacrificed in accordance with experimental protocols, which were reviewed and approved by the Animal Ethical Committee of The University of Trento and the Italian Ministry of Health.

For antibody titer analysis, CD1 mice were immunized intraperitoneally (i.p.) on days 0, 14 and 28 with 5 µg of OMVs from *E. coli* BL21(DE3)Δ58 or Δ60 strain transformed with pET-lpp-fhuD2, pET-lpp-Luke, pET-lpp-SpA, pET-lpp-FhuD2 hFat1 3x plasmid. Mice blood was collected through cardiac puncture at day 35 and serum was obtained from blood through centrifugation at 2,000 rpm for 10 minutes. Pools were obtained by mixing equal volumes of sera from mice immunized with the same type of OMVs and then they were used to perform ELISA experiments.

For T cell generation, BALB/c mice were i.p. injected on days 0 and 7 with 10 µg of OVA engineered OMVs derived from *E. coli* BL21(DE3)Δ58 or Δ60 strain. On day 12 spleens were collected and used for to perform intracellular cytokine staining analyzed.

## 9.11 ELISA

ELISA was performed using ninety-six well plates coated with 200 ng/well of FhuD2, Luke, SpA recombinant protein or using Nunc Immobilizer Amino plates (Thermo Fisher Scientific) plates coated with 200 ng/well of D8-FAT peptide, IQVEATDKDLGPNHGHTYSIVTDTD (Genescript). The day after, plates were washed 3 times with PBST (0.05% Tween 20 dissolved in PBS), saturated with 100 µl/plate of 1% BSA dissolved in PBS for 1 hour at 37°C and washed again 3 times with PBST. An equal amount of serum was added to the wells. Serum samples were initially diluted 1:300 in 1% BSA in PBS and then serial dilutions of 3-fold were performed. Serum samples were incubated for 1 hour at 37°C. Wells were subsequently washed 3 times with PBST and incubated for 1 hour at 37°C with alkaline phosphatase-conjugated goat α-mouse total IgG (Sigma-Aldrich) at a final dilution of 1:2,000. After triple PBST wash, 100 µl of Alkaline Phosphatase substrate (Sigma-Aldrich) were added to each well and plates were

maintained at RT in the dark for 30'. Finally, absorbance was read at 405nm using Tecan Infinite M200Pro Plate reader.

### 9.12 Intracellular cytokine staining on splenocytes

Spleens were homogenized and splenocytes filtered using a 70  $\mu$ m cell Strainer (BD). After centrifugation at 400 x g for 7', splenocytes were resuspended in RPMI+10%FBS and PSG and aliquoted in a 96-well plate at a concentration of  $1 \times 10^6$  cells per well. Cells were stimulated with 2 mg/ml of OVA peptide. As positive and negative controls, cells were stimulated with phorbol 12-myristate 13-acetate (PMA, 0.5 mg/ml) and Ionomycin (1 mg/ml) or with 2 mg/ml of an unrelated peptide, respectively. After 2 hours of stimulation at 37°C, Brefeldin A (BD) was added to each well and cells incubated for 4 hours at 37°C. After two washes with PBS, LIVE/DEAD™ Fixable Near-IR Dead Cell Stain Kit (Thermo Fisher Scientific) was incubated with the splenocytes for 20' at RT in the dark. After two washes with PBS and permeabilization and fixing with Cytotfix/Cytoperm (BD) following manufacturer's protocol, Fc receptors were blocked with 3  $\mu$ l of  $\alpha$ -CD16/CD32 for 15' at room temperature. Splenocytes were stained with the following fluorescent-labeled antibodies:  $\alpha$ -CD3-APC (BioLegend),  $\alpha$ -CD4-BV510 (BioLegend),  $\alpha$ -CD8-PECF594 (BD), and  $\alpha$ -IFN- $\gamma$ -BV785 (BioLegend). Samples were acquired on a BD FACSCanto II flow cytometer. Briefly, after gating lymphocytes from all events on the basis of SSC-A and FSC-A, single cells were selected on SSC-A and SSC-W, excluding both duplets and aggregates, which would have bound more and in a nonspecific manner, respectively, the antibodies. Live cells were selected as negative to LIVE/DEAD™ Fixable Near-IR Dead Cell Stain Kit (Thermo Fisher Scientific) and T lymphocytes were selected for CD3 expression. CD4 and CD8 lymphocytes were identified as positive for CD4 and CD8 molecules, respectively. IFN- $\gamma$  positive T cells were finally visualized against CD4 or CD8 expression (depending on the epitope nature), gating on the CD3 positive population. The IFN- $\gamma$  releasing CD4 and CD8 T cell populations were calculated as percentage of IFN- $\gamma$ /CD4 and IFN- $\gamma$ /CD8 double positive cells on the total of CD4 or CD8 cells, respectively. Graphs were performed with GraphPad Prism 5.03.

## 10 References

1. Cary P. Gross, MD;\* and Kent A. Sepkowitz, M. The myth of the Medical Breakthrough: smallpox, Vaccination, and Jenner Reconsidered. *Int. J. Infect. Dis.* **3**, 54–60 (1998).
2. Biggs, P. M. Gordon memorial lecture: Vaccines and vaccination—past, present and future. *Br. Poult. Sci.* **31**, 3–22 (1990).
3. STEFAN RIEDEL, MD, P. Edward Jenner and the history of smallpox and vaccination. 21–25 (2005). doi:10.1080/08998280.2005.11928028
4. Lakhani, S. Early clinical pathologists: Edward Jenner. *Clin Pathol* **45**, 756–758 (1992).
5. Plotkin, S. A. Vaccines: Past, present and future. *Nat. Med.* **11**, S5 (2005).
6. Plotkin, S. History of vaccination. *Proc. Natl. Acad. Sci.* **111**, 12283–12287 (2014).
7. KATZ SL, KEMPE CH, BLACK FL, LEPOW ML, KRUGMAN S, HAGGERTY RJ, E. J. Studies on an attenuated measles-virus vaccine. VIII. General summary and evaluation of the results of vaccination. *Am J Dis Child* **100**, 942–94 (1960).
8. Hilleman MR, Buynak EB, Weibel RE, Stokes J, J. Live, attenuated mumps-virus vaccine. *N Eng. J Med* **278(5)**:, 227–232
9. Plotkin SA, Farquhar JD, Katz M, B. F. Attenuation of RA 27-3 rubella virus in WI-38 human diploid cells. *Am J Dis Child* **118(2):178**, (1969).
10. Takahashi M, Okuno Y, Otsuka T, Osame J, T. A. Development of a live attenuated varicella vaccine. *Biken J. Mar*, 25–33 (1975).
11. Grandi, A., Tomasi, M. & Grandi, G. Vaccinology: The art of putting together the right ingredients. *Hum. Vaccines Immunother.* **12**, 1311–1317 (2016).
12. Iwasaki, A. & Medzhitov, R. Inmunidad Innata. *Nat. Immunol.* **16**, 343–353 (2015).
13. Delves, P. J. & Roitt, I. M. The immune system - Second of two parts. *N. Engl. J. Med.* **343**, 108–17 (2000).
14. Lim, K. & Staudt, L. M. Toll-Like Receptor Signaling. *Cold spring Harb. Perspect. Biol.* **5**, 5–7 (2013).
15. Gao, D. & Li, W. Structures and recognition modes of toll-like receptors. *Proteins* **85**, 3–9 (2016).
16. Siegrist, C. Vaccine Immunology. doi:10.1016/B978-1-4557-0090-5.00004-5
17. Wells, C. *et al.* Harnessing Case Isolation and Ring Vaccination to Control Ebola. *PLoS Negl. Trop. Dis.* **9**, 1–13 (2015).
18. Brito, L. A. & O’Hagan, D. T. Designing and building the next generation of improved vaccine adjuvants. *J. Control. Release* **190**, 563–579 (2014).
19. Kool, M. *et al.* Cutting Edge: Alum Adjuvant Stimulates Inflammatory Dendritic Cells through Activation of the NALP3 Inflammasome. *J. Immunol.* **181**, 3755–3759 (2014).
20. Day, W. C. Proceedings of the Chemical Section, of the Franklin Institute. *J. Franklin Inst.* **129**, 337–338 (1890).
21. Rappuoli, R., Pizza, M., Del Giudice, G. & De Gregorio, E. Vaccines, new opportunities for a new society. *Proc. Natl. Acad. Sci.* **111**, 12288–12293 (2014).
22. O’Hagan, D. T., Ott, G. S., Van Nest, G., Rappuoli, R. & Del Giudice, G. The history of MF59® adjuvant: A phoenix that arose from the ashes. *Expert Rev. Vaccines* **12**, 13–30 (2013).
23. O’Hagan, D. T. MF59 is a safe and potent vaccine adjuvant that enhances protection against influenza virus infection. *Expert Rev. Vaccines* **6**, 699–710 (2007).
24. Giudice, G. Del, Rappuoli, R. & Didierlaurent, A. M. Seminars in Immunology Correlates of adjuvanticity : A review on adjuvants in licensed vaccines. *Semin. Immunol.* **39**, 14–21 (2018).
25. Rachel Skinner, S. *et al.* Human papillomavirus (HPV)-16/18 AS04-adjuvanted vaccine for the prevention of cervical cancer and HPV-related diseases. *Expert Rev. Vaccines* **15**, 367–387 (2016).

26. De Gregorio, E., Caproni, E. & Ulmer, J. B. Vaccine adjuvants: Mode of action. *Front. Immunol.* **4**, 1–6 (2013).
27. Vermaelen, K. Vaccine Strategies to Improve Anti-cancer Cellular Immune Responses. *Front. Immunol.* **10**, 8 (2019).
28. Dubensky, T. W., Kanne, D. B. & Leong, M. L. Rationale, progress and development of vaccines utilizing STING-activating cyclic dinucleotide adjuvants. *Ther. Adv. Vaccines* **1**, 131–143 (2013).
29. Vance, D. L. B. & R. E. STING and the innate immune response to nucleic acids in the cytosol. *Nat. Immunol.* **2012**, *Revi*, 19–26 (2012).
30. Temizoz, B., Kuroda, E. & Ishii, K. J. Combination and inducible adjuvants targeting nucleic acid sensors. *Curr. Opin. Pharmacol.* **41**, 104–113 (2018).
31. Kulp, A. & Kuehn, M. J. Biological Functions and Biogenesis of Secreted Bacterial Outer Membrane Vesicles. *Annu Rev Microbiol* **64**, 163–184 (2010).
32. Jan, A. T. Outer Membrane Vesicles (OMVs) of gram-negative bacteria: A perspective update. *Front. Microbiol.* **8**, 1–11 (2017).
33. D. Mayrand, D. G. Biological activities of outer membrane vesicles. *Can. J. Microbiol.* **6**, 607–13 (1989).
34. Ellis, T. N. & Kuehn, M. J. Virulence and Immunomodulatory Roles of Bacterial Outer Membrane Vesicles. *Microbiol. Mol. Biol. Rev.* **74**, 81–94 (2010).
35. Alaniz, R. C. *et al.* Membrane Vesicles Are Immunogenic Facsimiles of Salmonella typhimurium That Potently Activate Dendritic Cells, Prime B and T Cell Responses, and Stimulate Protective Immunity In Vivo. *J. Immunol.* **179**, 7692–7701 (2007).
36. Collins, B. S. Gram-negative outer membrane vesicles in vaccine development. *Discov. Med.* **12**, 7–15 (2011).
37. Schild, S., Nelson, E. J., Bishop, A. L. & Camilli, A. Characterization of Vibrio cholerae outer membrane vesicles as a candidate vaccine for cholera. *Infect. Immun.* **77**, 472–484 (2009).
38. Marzia M. Giuliani\* *et al.* A Universal Vaccine for Serogroup B Meningococcus. *PNAS* **103**, 10834–10839 (2006).
39. Needham, B. D., Carroll, S. M., Giles, D. K., Georgiou, G. & Whiteley, M. Modulating the innate immune response by combinatorial engineering of endotoxin. *PNAS* **110**, 1464–1469 (2013).
40. Cecil, J. D. *et al.* Outer membrane vesicles prime and activate macrophage inflammasomes and cytokine secretion in vitro and in vivo. *Front. Immunol.* **8**, 1–22 (2017).
41. Manuscript, A. & Vesicles, O. M. Incorporation of Heterologous Outer Membrane and Periplasmic Proteins into Escherichia coli Outer Membrane Vesicles. **279**, 2069–2076 (2012).
42. Jae-Young Kim<sup>1</sup>, Anne M. Doody<sup>1</sup>, David J. Chen, Gina H. Cremona, David Putnam<sup>1</sup>, and M. P. D. Engineered bacterial outer membrane vesicles with enhanced functionality. *J Mol Biol* **380**, 51–66 (2008).
43. Fantappiè, L. *et al.* Antibody-mediated immunity induced by engineered in their lumen coli OMVs carrying heterologous antigens. **1**, 1–14 (2014).
44. Fantappiè, L. *et al.* Some gram-negative lipoproteins keep their surface topology when transplanted from one species to another and deliver foreign polypeptides to the bacterial surface. *Mol. Cell. Proteomics* **16**, 1348–1364 (2017).
45. Deatherage, B. L. *et al.* Biogenesis of Bacterial Membrane Vesicles. *Mol Microb.* **72**, 1395–1407 (2010).
46. Bernadac, A., Gavioli, M., Lazzaroni, J., Raina, S. & Inge, L. Escherichia coli tol-pal Mutants Form Outer Membrane Vesicles. *J. Bacteriol.* **180**, 4872–4878 (1998).
47. Scorza, F. B. *et al.* High Yield Production Process for Shigella Outer Membrane Particles. *PLoS One* **7**, 1–15 (2012).
48. Choi, K.-H. *et al.* Outer Membrane Vesicles Derived from Escherichia coli Induce Systemic Inflammatory Response Syndrome. *PLoS One* **5**, 1–6 (2010).

49. Somerville, J. E., Cassiano, L., Bainbridge, B., Cunningham, M. D. & Darveau, R. P. A Novel *Escherichia coli* Lipid A Mutant That Produces an Antiinflammatory Lipopolysaccharide. *J. Clin. Invest.* **97**, 359–365 (1996).
50. Bishop, R. E. *et al.* Transfer of palmitate from phospholipids to lipid A in outer membranes of Gram-negative bacteria. *EMBo J.* **19**, 5071–5080 (2000).
51. Altindis, E., Fu, Y. & Mekalanos, J. J. Proteomic analysis of *Vibrio cholerae* outer membrane vesicles. *Proc. Natl. Acad. Sci.* **111**, E1548–E1556 (2014).
52. Lee, E. Y. *et al.* Global proteomic profiling of native outer membrane vesicles derived from *Escherichia coli*. *Proteomics* **7**, 3143–3153 (2007).
53. Toloza, L. *et al.* Proteomic analysis of outer membrane vesicles from the probiotic strain *Escherichia coli* Nissle 1917. *Proteomics* **14**, 222–229 (2013).
54. Zhang, Y., Buchholz, F., Muyrers, J. P. P. & Francis Stewart, A. A new logic for DNA engineering using recombination in *Escherichia coli*. *Nat. Genet.* **20**, 123–128 (1998).
55. Datta, S., Costantino, N. & Court, D. L. A set of recombinering plasmids for gram-negative bacteria. **379**, 109–115 (2006).
56. Murphy, K. C.  $\lambda$  Recombination and Recombineering. *EcoSal Plus* **7**, 1–70 (2016).
57. Muyrers, J. P. P., Zhang, Y., Testa, G. & Stewart, A. F. Rapid modification of bacterial artificial chromosomes by ET-recombination. **27**, 1555–1557 (1999).
58. Yang, J. *et al.* High-efficiency scarless genetic modification in *Escherichia coli* by using lambda red recombination and I-SceI cleavage. *Appl. Environ. Microbiol.* **80**, 3826–3834 (2014).
59. Yu, D., Sawitzke, J. A., Ellis, H. & Court, D. L. Recombineering with overlapping single-stranded DNA oligonucleotides: Testing a recombination intermediate. **100**, 7207–7212 (2003).
60. Jiang, W. & Marraffini, L. A. CRISPR-Cas: New Tools for Genetic Manipulations from Bacterial Immunity Systems. *Annu. Rev. Microbiol.* **69**, 209–228 (2015).
61. Standage-Beier, K., Zhang, Q. & Wang, X. Targeted Large-Scale Deletion of Bacterial Genomes Using CRISPR-Nickases. *ACS Synth. Biol.* **4**, 1217–1225 (2015).
62. Reisch, C. R. & Prather, K. L. J. The no-SCAR (Scarless Cas9 Assisted Recombineering) system for genome editing in *Escherichia coli*. *Sci. Rep.* **5**, 15096 (2015).
63. Li, Y. *et al.* Metabolic engineering of *Escherichia coli* using CRISPR–Cas9 mediated genome editing. *Metab. Eng.* **31**, 13–21 (2015).
64. Wenyan Jiang, David Bikard, David Cox, Feng Zhang, L. A. M. CRISPR-assisted editing of bacterial genomes. *Nat biotechnol* **31**, 233–239 (2013).
65. Derbise, A., Lesic, B., Dacheux, D., Marc, J. & Carniel, E. A rapid and simple method for inactivating chromosomal genes in *Yersinia*. **38**, 113–116 (2003).
66. Gay, P., Cqq, D. L. E., Steinmetz, M., Berkelman, T. & Kadol, C. I. Positive Selection Procedure for Entrapment of Insertion Sequence Elements in Gram-Negative Bacteria. *J. Bacteriol.* **164**, 918–921 (1985).
67. Whitfield, C. R. H. R. and C. Lipopolysaccharide Endotoxins. *Annu Rev Biochem* **71**, 635–700 (2002).
68. Del Vecchio, C. A., Li, G. & Wong, A. J. Targeting EGF receptor variant III: Tumor-specific peptide vaccination for malignant gliomas. *Expert Rev. Vaccines* **11**, 133–144 (2012).
69. Parri, M. *et al.* FAT1: a potential target for monoclonal antibody therapy in colon cancer. *Br. J. Cancer* **115**, 40–51 (2016).
70. Pyne, M. E., Moo-Young, M., Chung, D. A. & Chou, C. P. Coupling the CRISPR/Cas9 system with lambda red recombineering enables simplified chromosomal gene replacement in *Escherichia coli*. *Appl. Environ. Microbiol.* **81**, 5103–5114 (2015).
71. Jiang, Y. *et al.* Multigene editing in the *Escherichia coli* genome via the CRISPR–Cas9 system. *Appl. Environ. Microbiol.* **81**, 2506–2514 (2015).
72. Gay, P., Coq, D. L. E., Steinmetz, M., Ferrari, E. & Hoch, J. A. Cloning Structural Gene *sacB*, Which Codes for Exoenzyme Levansucrase of *Bacillus subtilis*: Expression of the Gene in *Escherichia coli*.

- 153**, 1424–1431 (1983).
73. Hale, L., Lazos, O., Haines, A. S. & Thomas, C. M. An efficient stress-free strategy to displace stable bacterial plasmids. *BioTechnique* **48**, 223–228 (2010).
  74. Roier, S. *et al.* A novel mechanism for the biogenesis of outer membrane vesicles in Gram-negative bacteria. *Nat. Commun.* **7**, 1–13 (2016).
  75. Grandi, A. *et al.* Vaccination With a FAT1-Derived B Cell Epitope Combined With Tumor-Specific B and T Cell Epitopes Elicits Additive Protection in Cancer Mouse Models. **8**, 1–14 (2018).
  76. Baba, T. *et al.* Construction of Escherichia coli K-12 in-frame , single-gene knockout mutants : the Keio collection. *Molecuclar Syst. Biol.* **4474**, 1–11 (2006).
  77. Zerbini, F. *et al.* Large scale validation of an efficient CRISPR/Cas-based multi gene editing protocol in Escherichia coli. *Microb. Cell Fact.* **16**, (2017).
  78. Koehn, J. *et al.* High Throughput Protein Expression and Purification. *Methods Mol. Biol.* **498**, 117–127 (2009).
  79. Murphy, K. C., Campellone, K. G. & Poteete, A. R. PCR-mediated gene replacement in Escherichia coli. *Gene* **246**, 321–330 (2000).
  80. Cesaratto, F., Burrone, O. R. & Petris, G. Tobacco Etch Virus protease: A shortcut across biotechnologies. *J. Biotechnol.* **231**, 239–249 (2016).

# 11 Publications

## **Vaccination With a FAT1-Derived B Cell Epitope Combined With Tumor-Specific B and T Cell Epitopes Elicits Additive Protection in Cancer Mouse Models.**

Grandi A, Fantappiè L, Irene C, Valensin S, Tomasi M, Stupia S, Corbellari R, Caproni E, **Zanella I**, Isaac SJ, Ganfini L, Frattini L, König E, Gagliardi A, Tavarini S, Sammicheli C, Parri M, Grandi G.  
Front Oncol. 2018 Oct 26;8:481.

*I personally contributed to perform flow cytometry, T cell analysis and tumor challenge.*

## **VSV-G-Enveloped Vesicles for Traceless Delivery of CRISPR-Cas9.**

Montagna C, Petris G, Casini A, Maule G, Franceschini GM, **Zanella I**, Conti L, Arnoldi F, Burrone OR, Zentilin L, Zacchigna S, Giacca M, Cereseto A.  
Mol Ther Nucleic Acids. 2018 Sep 7;12:453-462.

*I personally contributed to perform the experiments in cell lines.*

## **Synergistic Protective Activity of Tumor-Specific Epitopes Engineered in Bacterial Outer Membrane Vesicles.**

Grandi A, Tomasi M, **Zanella I**, Ganfini L, Caproni E, Fantappiè L, Irene C, Frattini L, Isaac SJ, König E, Zerbini F, Tavarini S, Sammicheli C, Giusti F, Ferlenghi I, Parri M, Grandi G.  
Front Oncol. 2017 Nov 7;7:253.

*I performed the animal studies, discussed the results and contributed to the manuscript writing.*

## **Some Gram-negative Lipoproteins Keep Their Surface Topology When Transplanted from One Species to Another and Deliver Foreign Polypeptides to the Bacterial Surface.**

Fantappiè L, Irene C, De Santis M, Armini A, Gagliardi A, Tomasi M, Parri M, Cafardi V, Bonomi S, Ganfini L, Zerbini F, **Zanella I**, Carnemolla C, Bini L, Grandi A, Grandi G.  
Mol Cell Proteomics. 2017 Jul;16(7):1348-1364.

*I personally contributed to the OMVs preparation and to the final version of the manuscript.*

## **Large scale validation of an efficient CRISPR/Cas-based multi gene editing protocol in Escherichia coli.**

Zerbini F, **Zanella I**, Fraccascia D, König E, Irene C, Frattini LF, Tomasi M, Fantappiè L, Ganfini L, Caproni E, Parri M, Grandi A, Grandi G.  
Microb Cell Fact. 2017 Apr 24;16(1):68.

*I designed and performed the experiments and analyzed the data. Moreover, I conceived the original idea and performed the experiments on the simultaneous genes deletion. Discussed the results and contributed to the manuscript writing.*

## **Design, Characterization, and Lead Selection of Therapeutic miRNAs Targeting Huntingtin for Development of Gene Therapy for Huntington's Disease.**

Miniarikova J, **Zanella I**, Huseinovic A, van der Zon T, Hanemaaijer E, Martier R, Koornneef A, Southwell AL, Hayden MR, van Deventer SJ, Petry H, Konstantinova P.  
Mol Ther Nucleic Acids. 2016 Mar 22;5:e297.

*I performed and analyzed the data of all the in vitro experiments related to the allele-specific silencing approach.*

## 12 Acknowledgments

Firstly, I would like to express my sincere gratitude to my advisor Prof. Guido Grandi. Thanks for the opportunity he gave me to spend my Ph.D. in his laboratory, for the scientific support and guidance during these years and for supporting me with the thesis writing.

Thanks also to all the people who were part of our laboratory during those years. Francesca who started the project, Enrico that was and is involved with me in this project, Carmela, Luca, Samine, Alvisè, Alberto, Assunta, Laura, Elena to be amazing colleagues and especially Mirel to be always ready to listen to me and cheer me up.

I would also thank Pavlina Kostantinova, my Master Student supervisor, who believed in my abilities and pushed me to enroll to the Ph.D. studies.

Thanks to my friends Caterina, Silvia and Diana to be present in the after working hours ready to forget failing experiments and celebrate good days with a glass of beer.

Last but not least, I would like to thank my family: my parents, my sister and my husband, for supporting me spiritually throughout writing this thesis and my life in general.